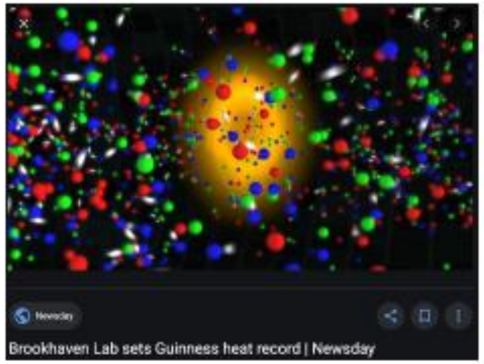

Hottest

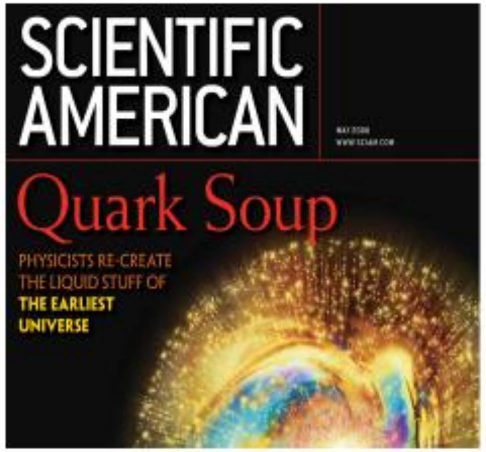

Least viscous

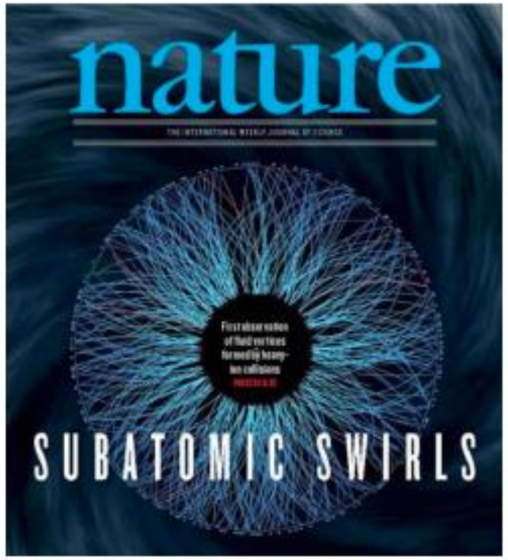

Most vortical

???

Supported in part by
U.S. DEPARTMENT OF ENERGY

Recent results from the STAR experiment

Alexey Aparin for the STAR collaboration
Joint Institute for Nuclear Research

Part of this work was supported by Russian Science Foundation under grant № 22-72-10028

STAR detector

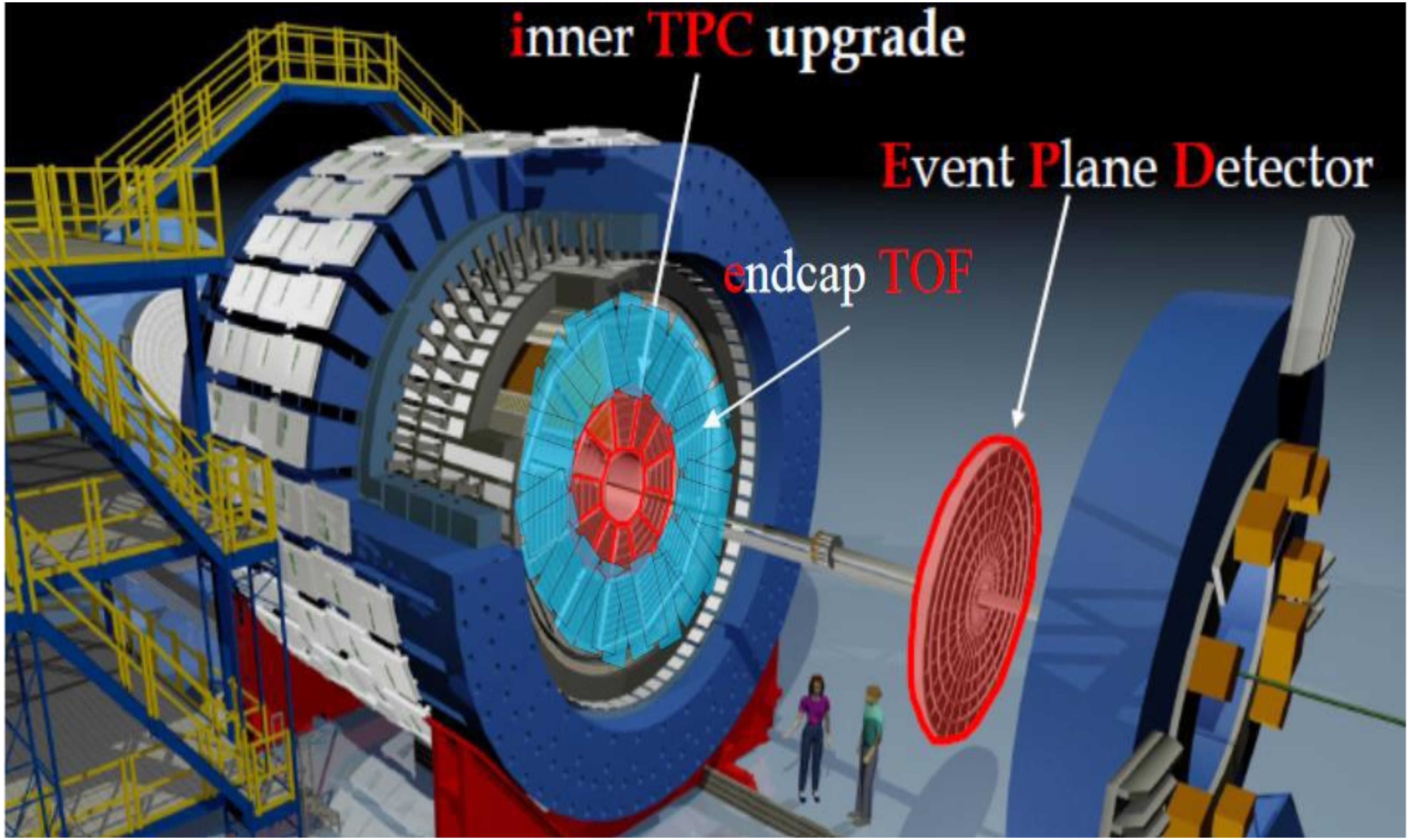

- **Tracking and PID (full 2π)**
  TPC: |η| < 1
  iTPC (2019+): |η| < 1.5
  TOF: |η| < 1
  eTOF (2019+): -1.6 < η < -1
  BEMC: |η| < 1
  EEMC: 1 < η < 2
  HFT (2014-2016): |η| < 1
  MTD (2014+): |η| < 0.5 (partial azimuthal coverage)

- **MB trigger and event plane reconstruction**
  BBC (before 2018): 3.3 < |η| < 5
  EPD (2018+): 2.1 < |η| < 5.1
  VPD: 4.2 < |η| < 5
  ZDC: 6.5 < |η| < 7.5

- **Recent upgrades 2022**
  FCS: 2.5 < |η| < 4
  FTS: 2.5 < |η| < 4
  ECAL & HCAL: 2.5 < |η| < 4

Top RHIC energy
Lattice QCD region

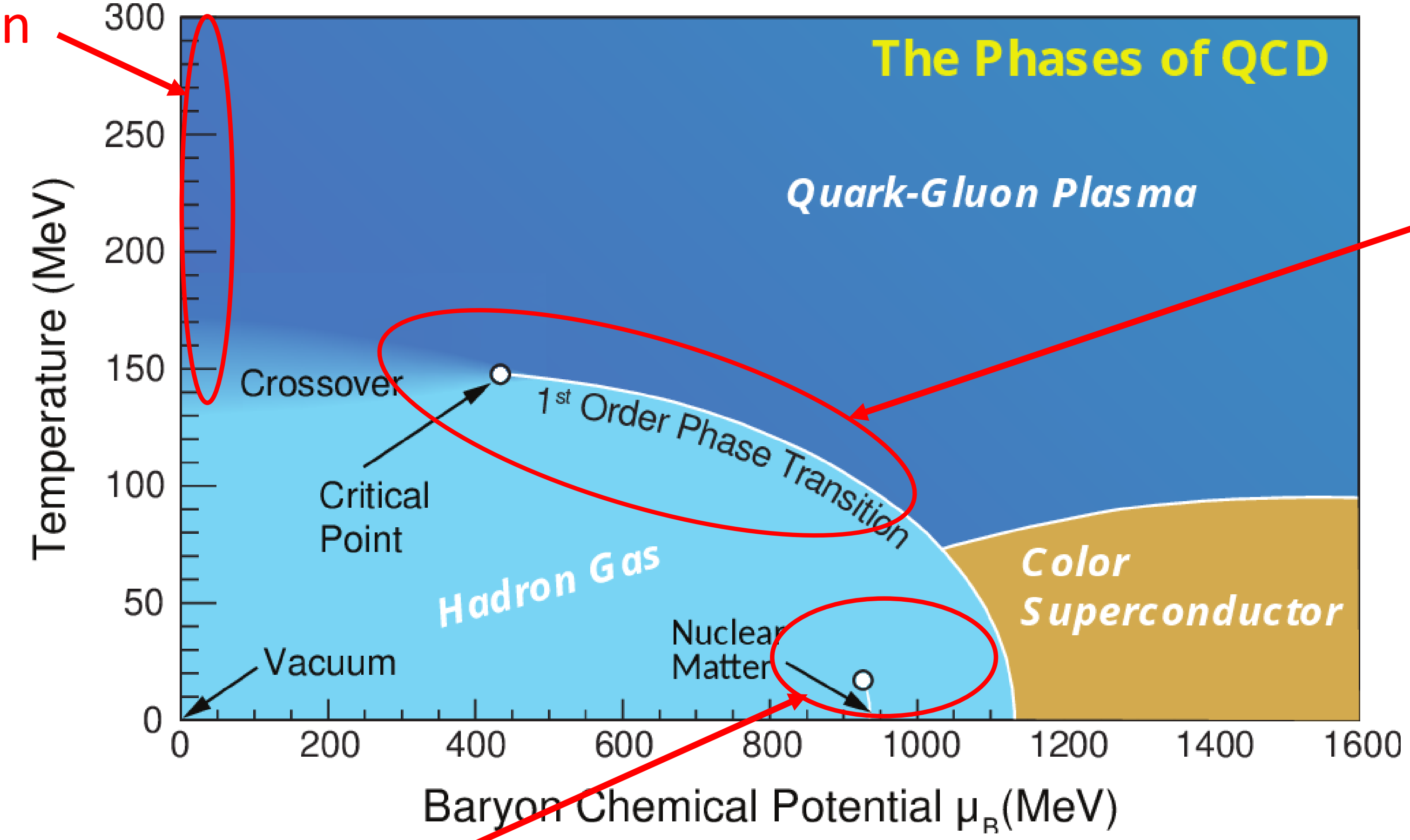

Beam energy scan
High density hot
QCD region

Cold QCD physics
High density region

Beam Energy Scan

Beam Energy Scan to map the QCD phase diagram

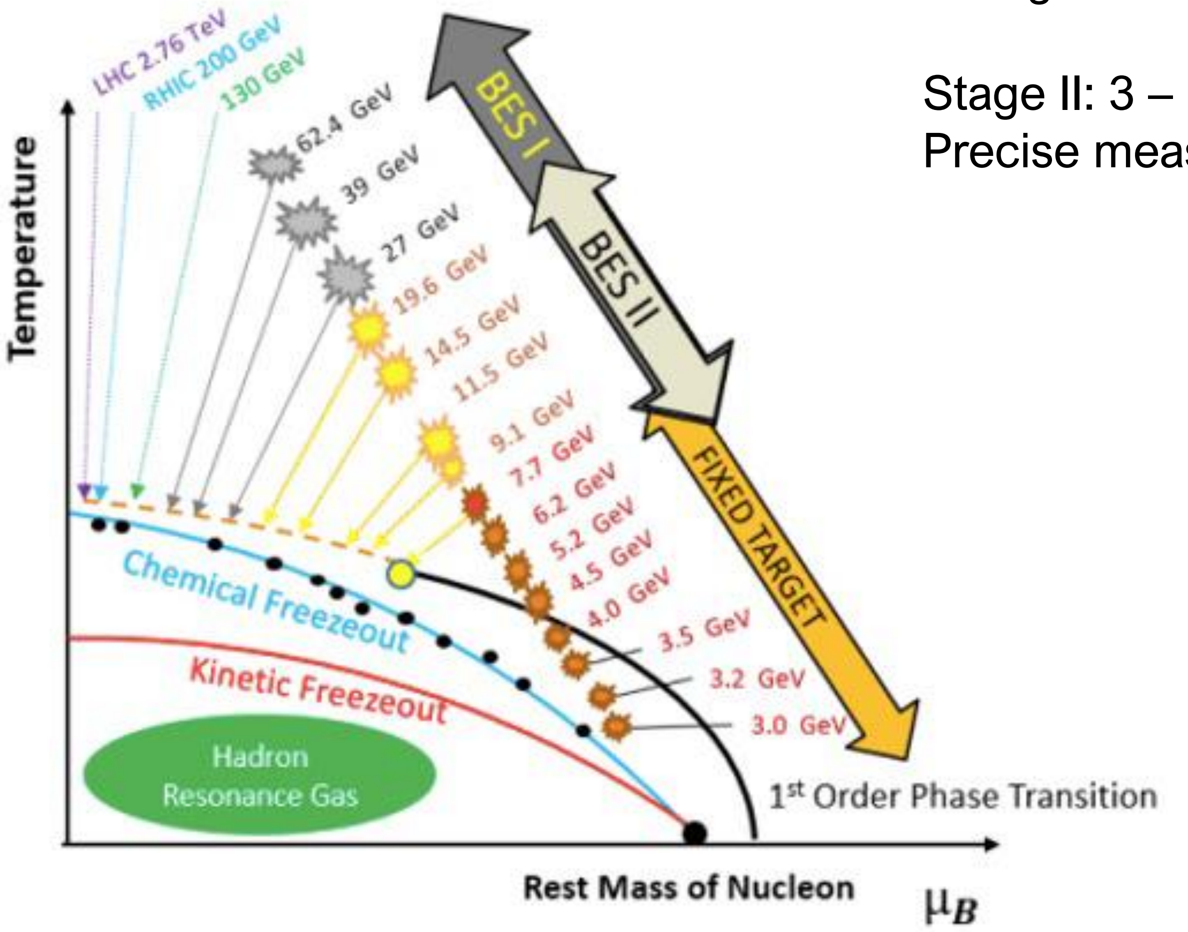

Two stages of Beam Energy Scan:
Stage I: 7.7 – 39 GeV 2010 – 2014
First glance at low energy region, rather low statistics

Stage II: 3 – 54.4 GeV 2017 – 2021
Precise measurements at low energies, large statistics

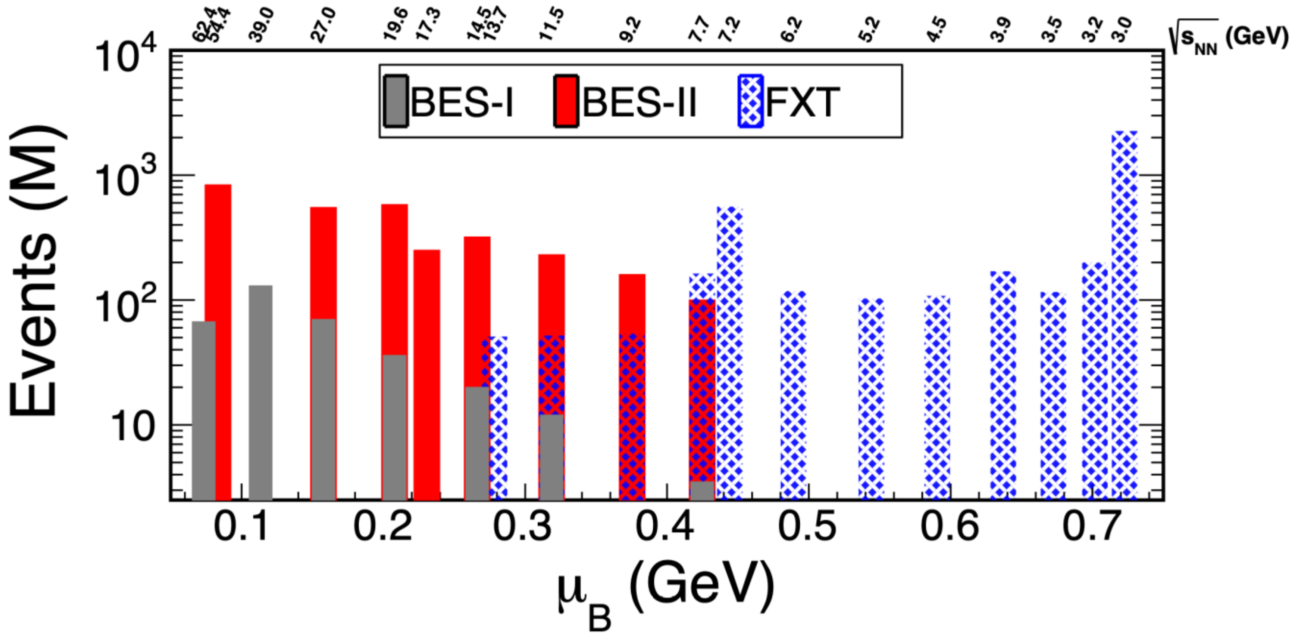

Light particle production at 27 GeV

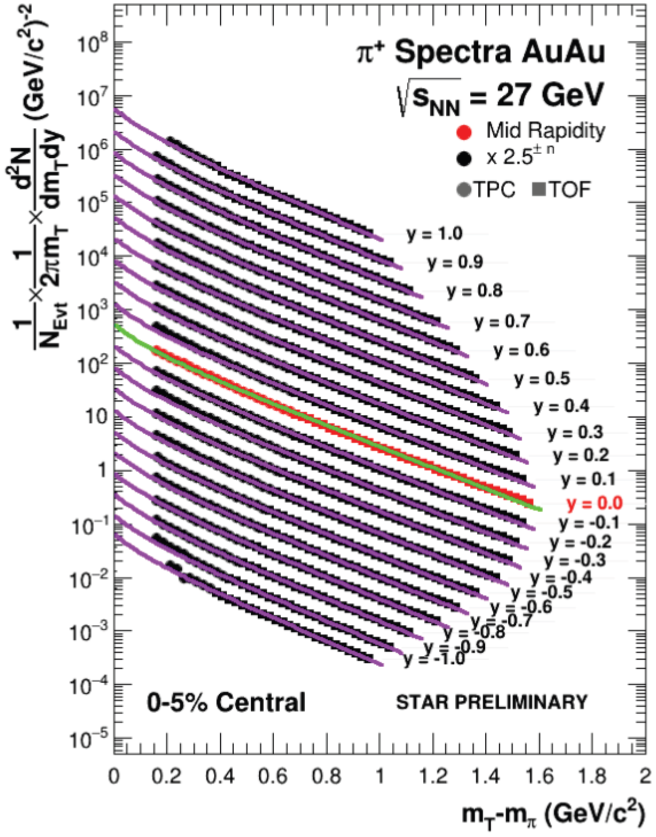

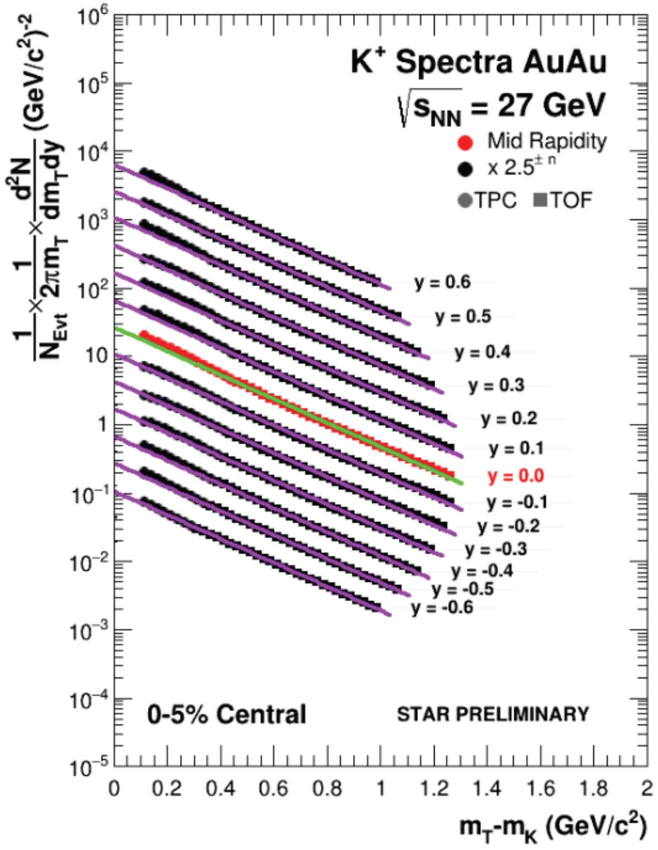

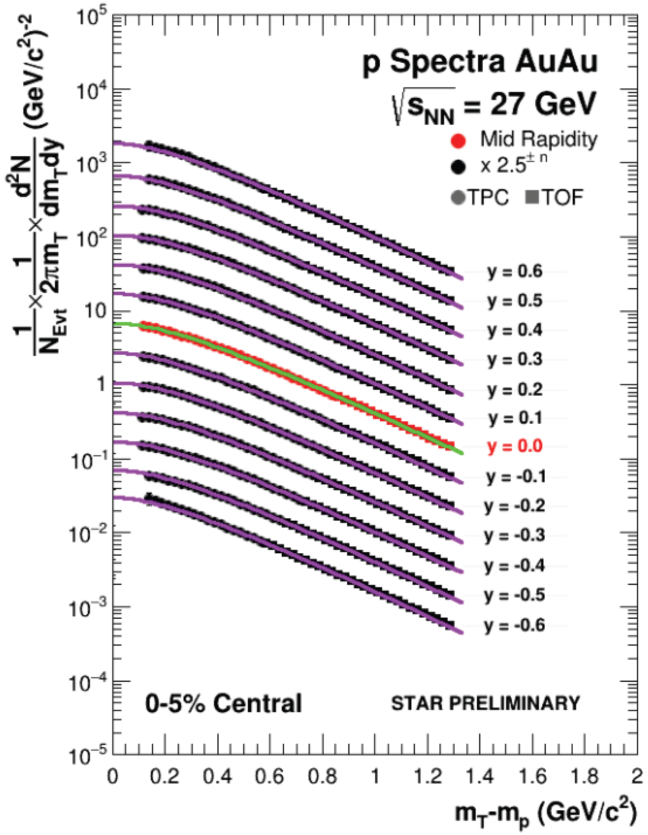

High statistics of BES-II allows to make a rapidity dependence study of particle production

With iTPC and eTOF upgrade more high precision data on particle production are on the way at lower energies

Thermodynamical properties of the medium

Similar rapidity dependence of the T_{chem} and μ_B, μ_S over particle multiplicity

Precise study of the QCD phase diagram location of the interaction at different collision energies

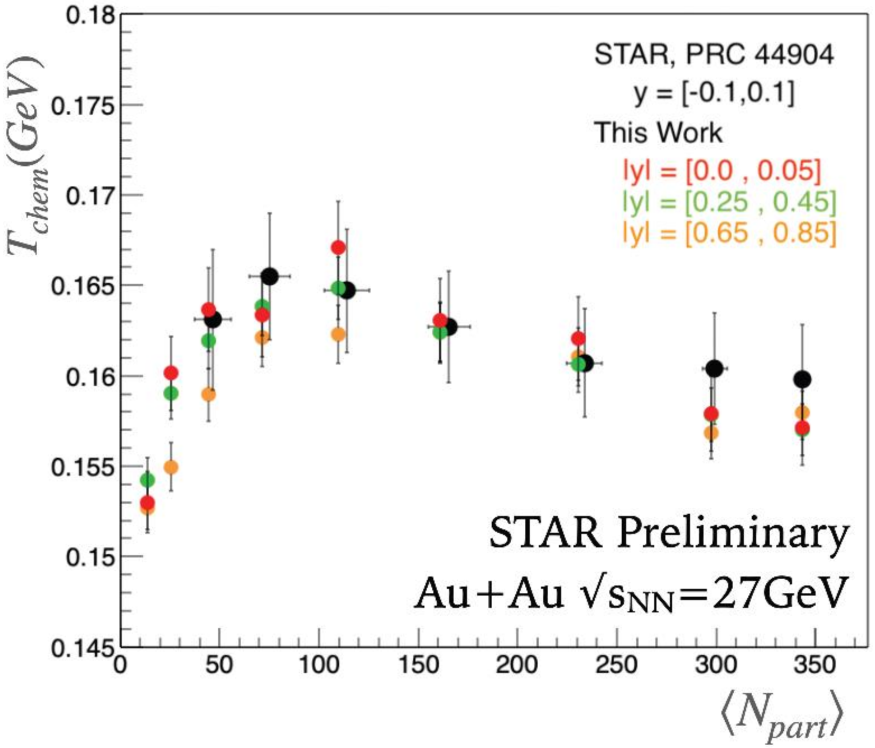

Fits by THERMUS Chemical equilibrium model

$\Delta\mu_B \approx 25$ MeV for $\Delta y = 1$ at 27 GeV

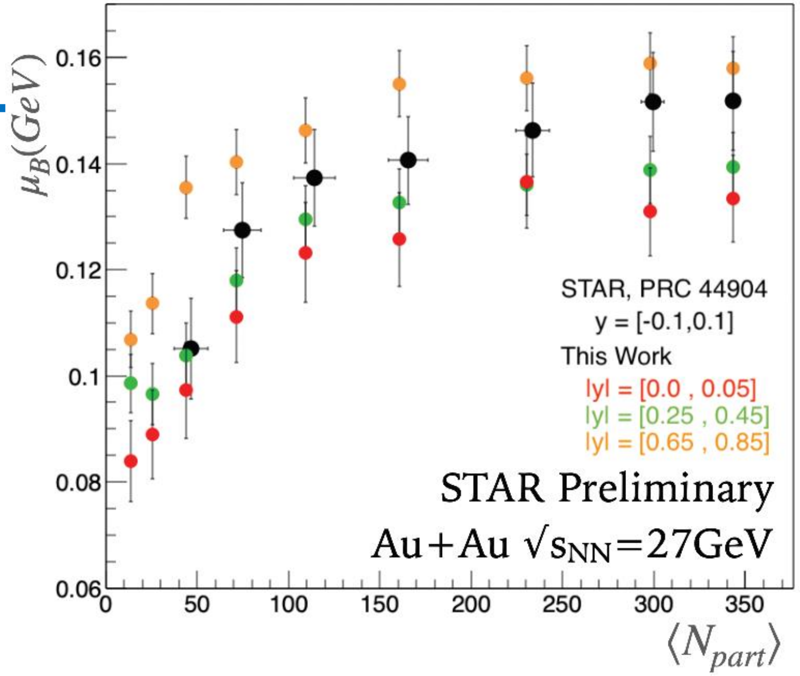

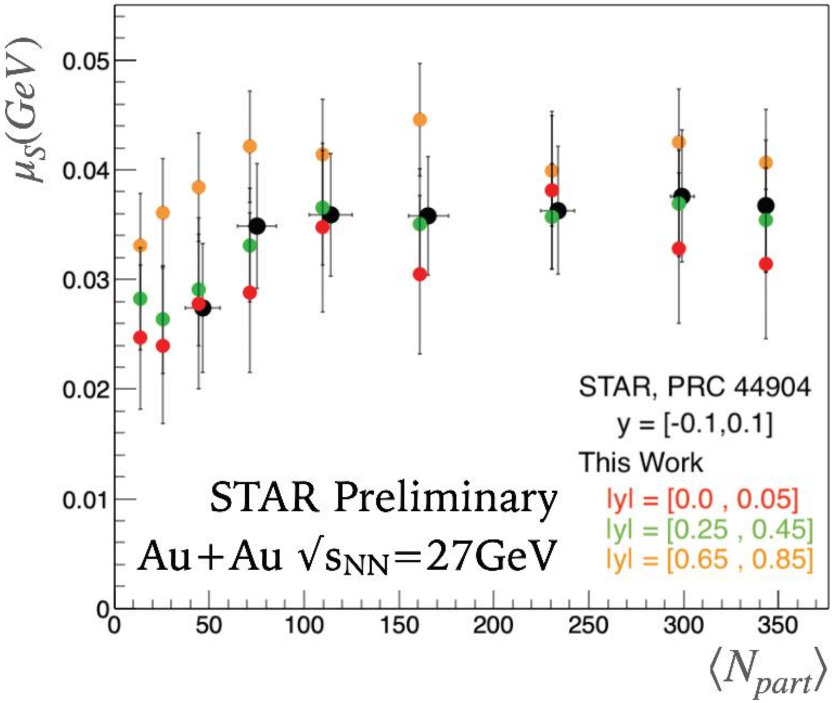

Nuclear modification in the medium

$$R_{cp} = \frac{d^2Ndp_t d\eta / < N_{coll} > (central)}{d^2Ndp_t d\eta / < N_{coll} > (peripheral)}$$

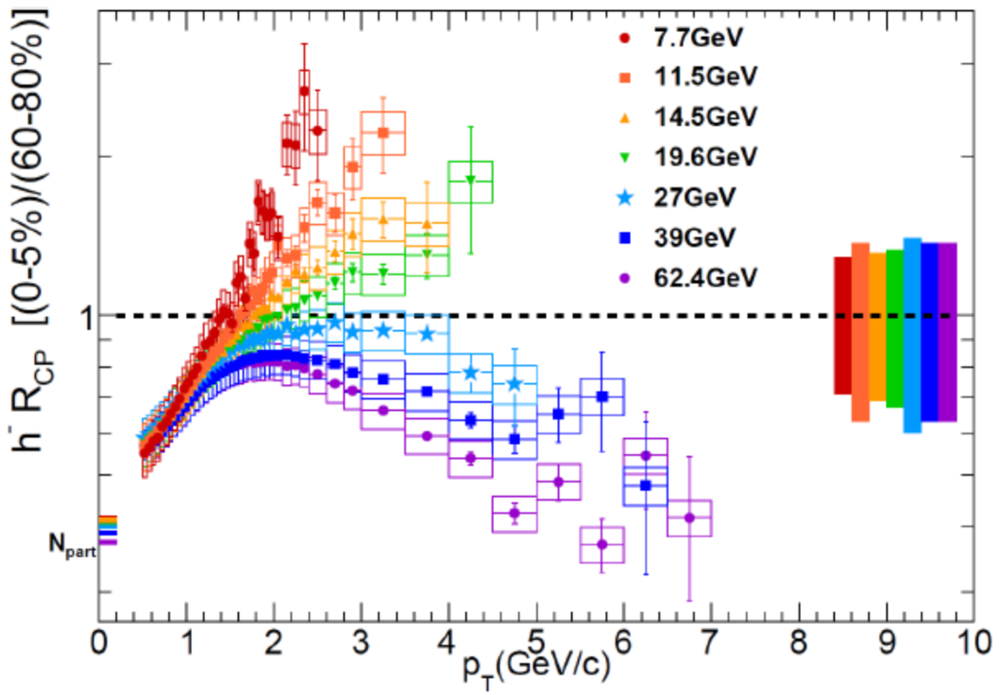

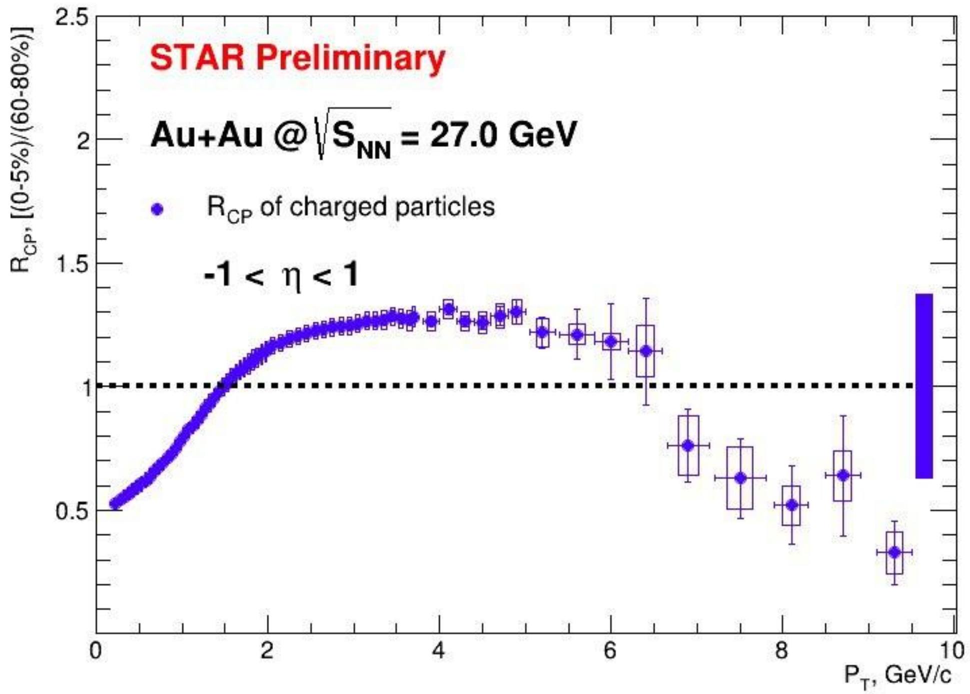

R_{cp} has two regimes in the behavior depending on the collision energy:
decrease of particle production with high p_T in central collisions at high energies
smooth growth of particle production in central collisions at low collision energies.
High statistics of BES-II will allow to measure R_{cp} in high p_T region at low collision energies

STAR Phys. Rev. C **102** (2020) 34909
STAR Phys. Rev. Lett. **121** (2018) 32301

Nuclear modification in the medium

$$\mathrm{R_{cp}} = \frac{d^2 N dp_t d\eta / < N_{coll} > (central)}{d^2 N dp_t d\eta / < N_{coll} > (peripheral)}$$

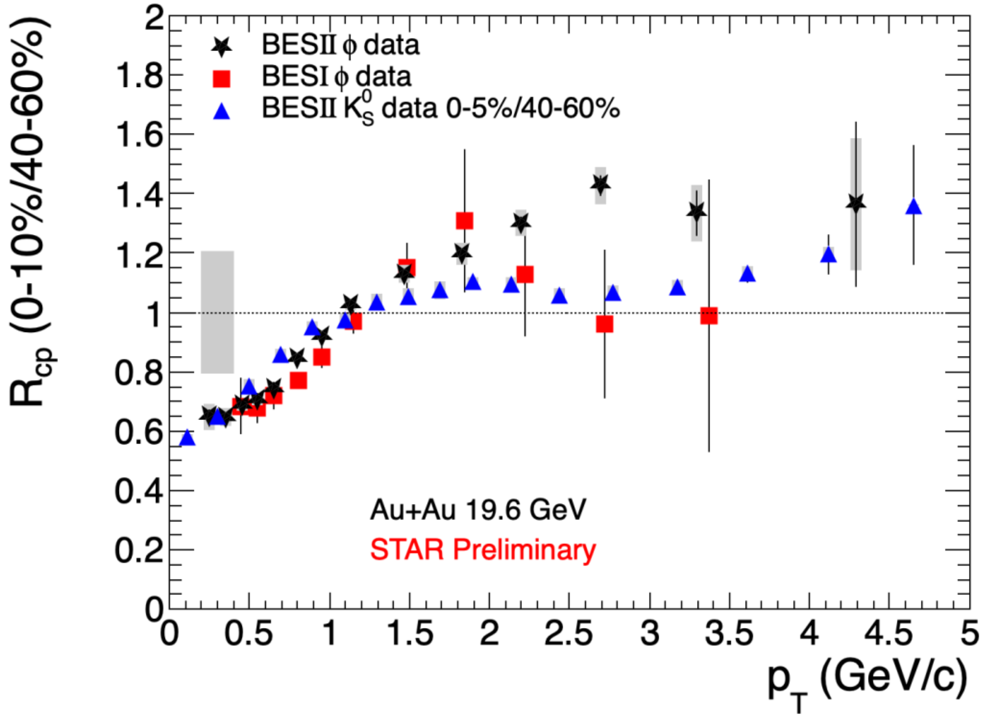

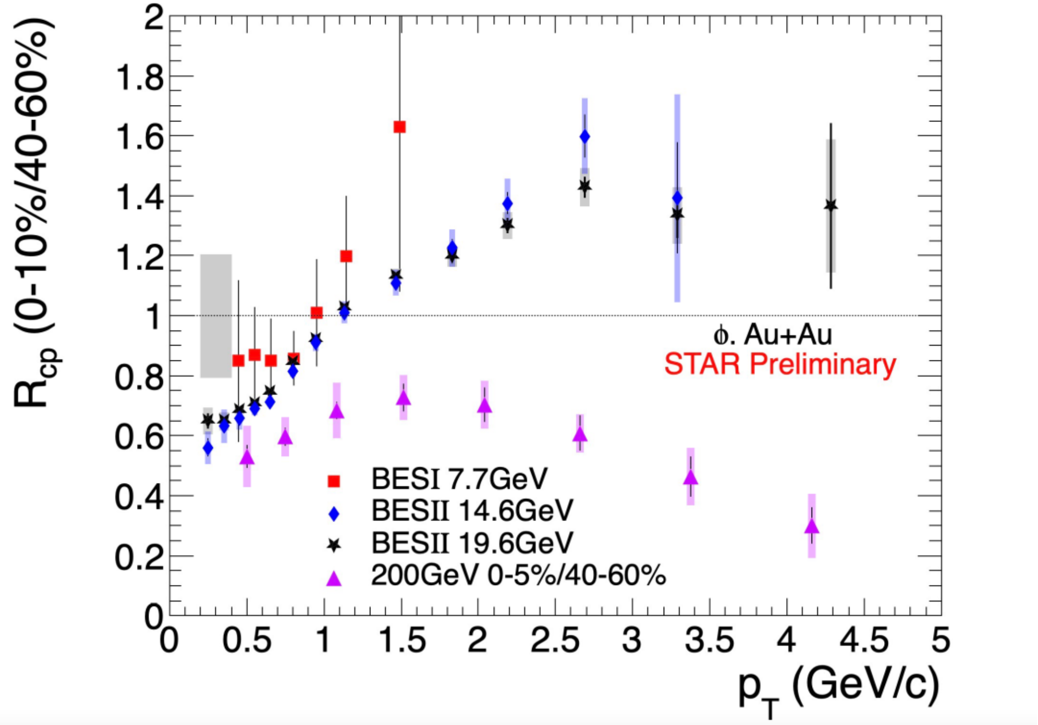

High statistics of BES-II allows to measure nuclear modification factor in high p_T region for different particles
Allows to compare different particle species which can be sensitive for different QGP effects

Collective flow of light nuclei

Collective flow of light nuclei demonstrates mass number dependence for BES-II collider energies

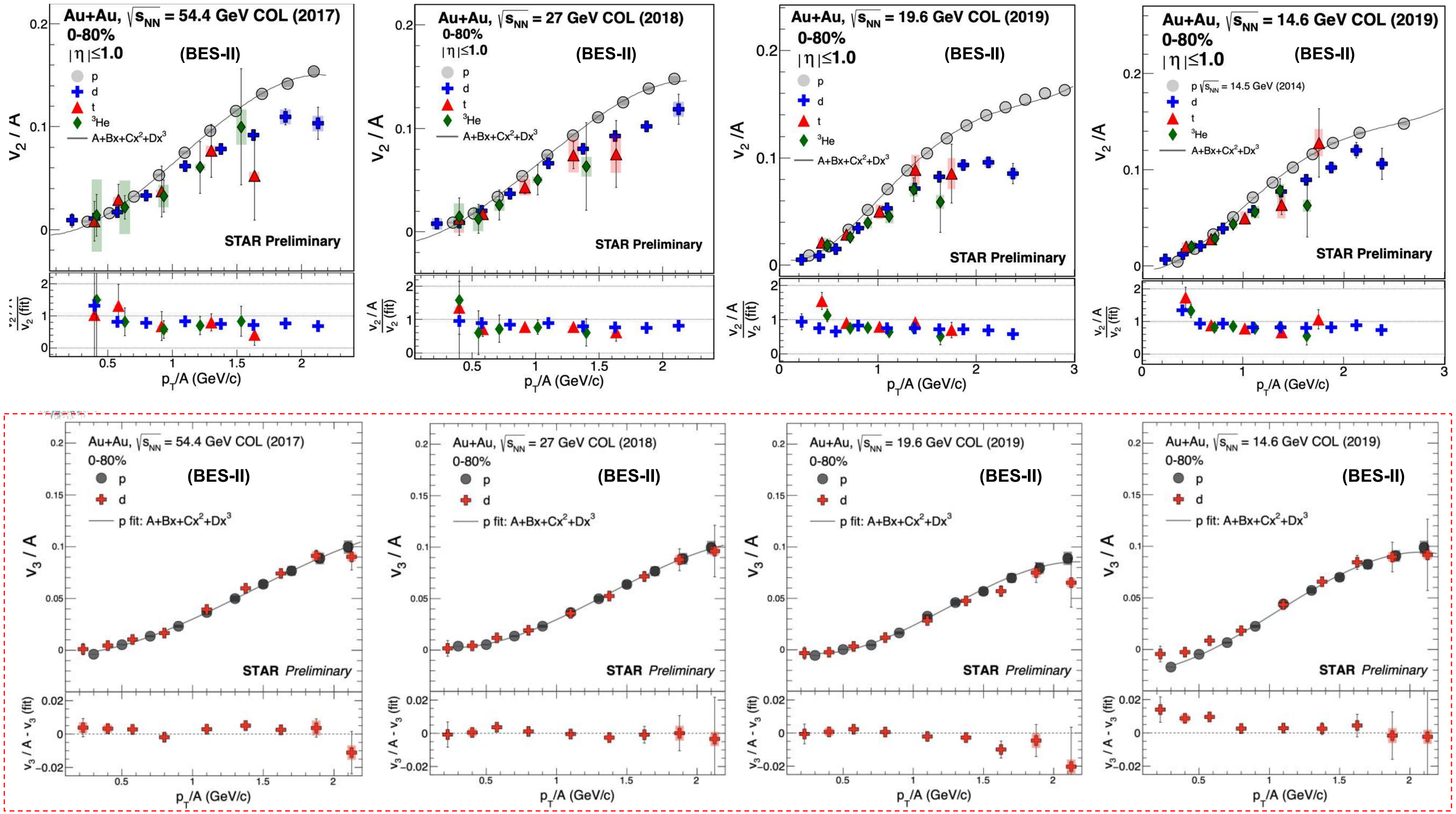

Scaling for light nuclei species for v_2/A and for v_3/A taking into account mass number of the nuclei was calculated

The A-scaling is observed for light nuclei v_3 but not for v_2

Collective flow of light nuclei

This indicates that no A scaling is observed in these data for light nucleus v_2 at 3 GeV.
Nucleon coalescence model qualitatively reproduce both the v_1 and v_2 as functions of rapidity for all investigated light nuclei at the energy, where baryonic interactions dominate the collision dynamic

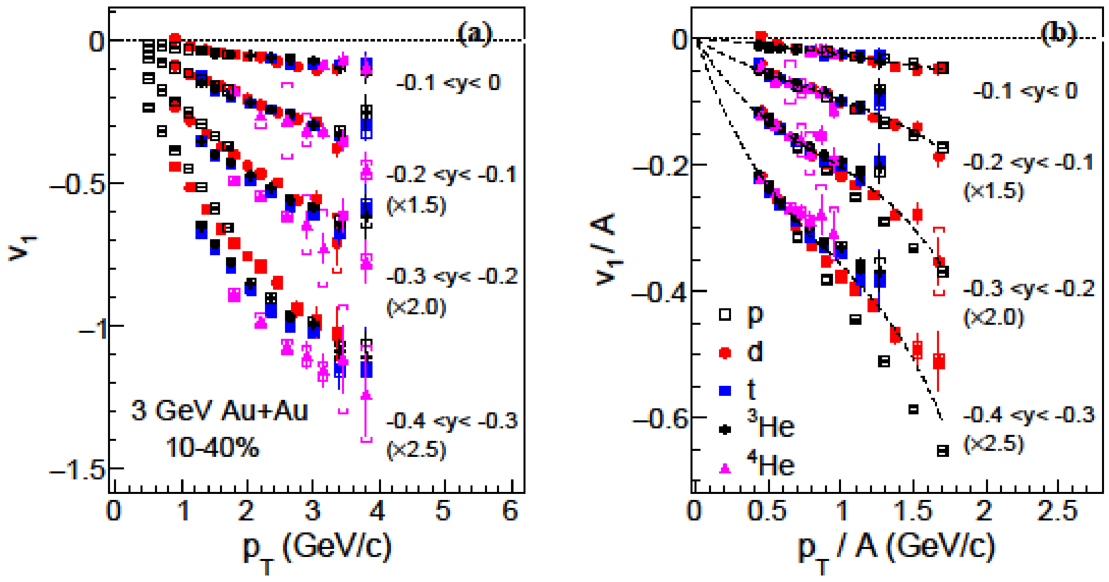

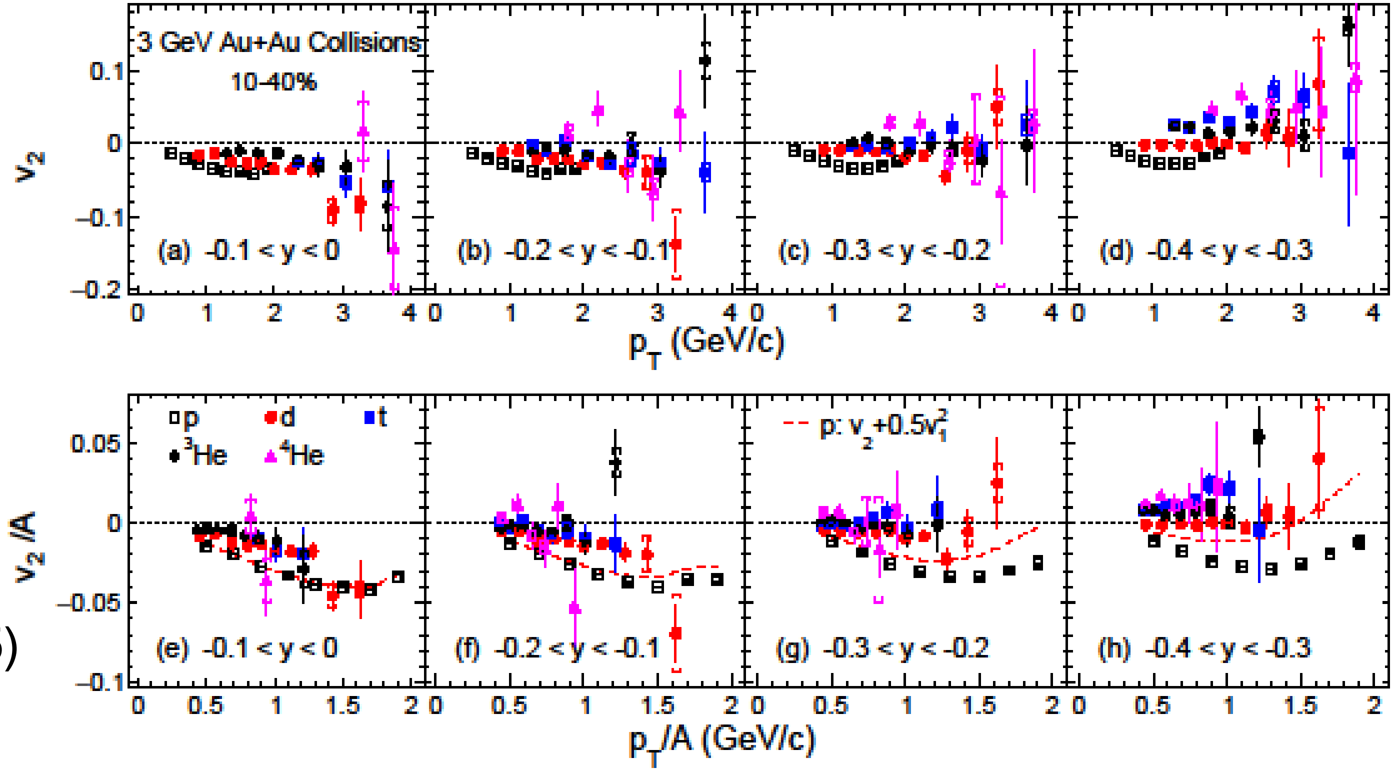

The v_1 scaling behavior suggests the light nuclei are formed via nucleon coalescence
The scaling worsens for $p_T/A > 1$ GeV/c in the range $-0.4 < y < -0.3$
Increasing contamination of target-rapidity ($y = -1.045$) fragments may also play a role

STAR Phys. Lett. B **827** (2022) 136941

Elliptic flow at low energies

Elliptic flow is negative (squeeze-out) at 3 GeV, as expected from the previous AGS data.
Grows rapidly with energy

The quark number scaling has been used at higher energies as a signature of the QGP. At 3 and 3.2 GeV, the scaling is broken down e.g. hadronic gas (not QGP)

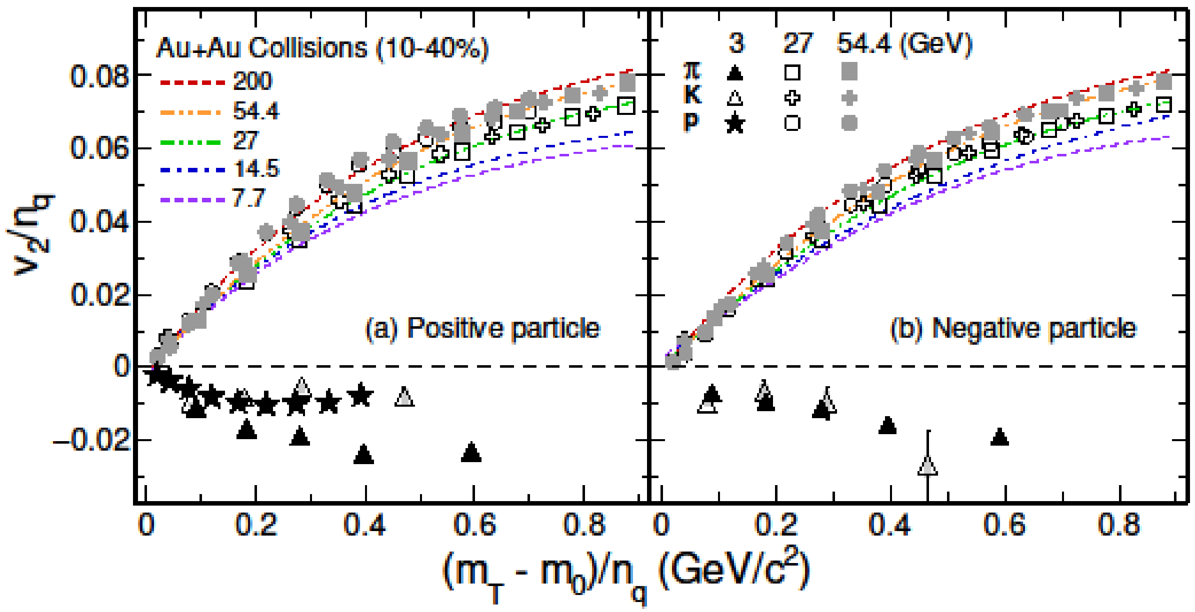

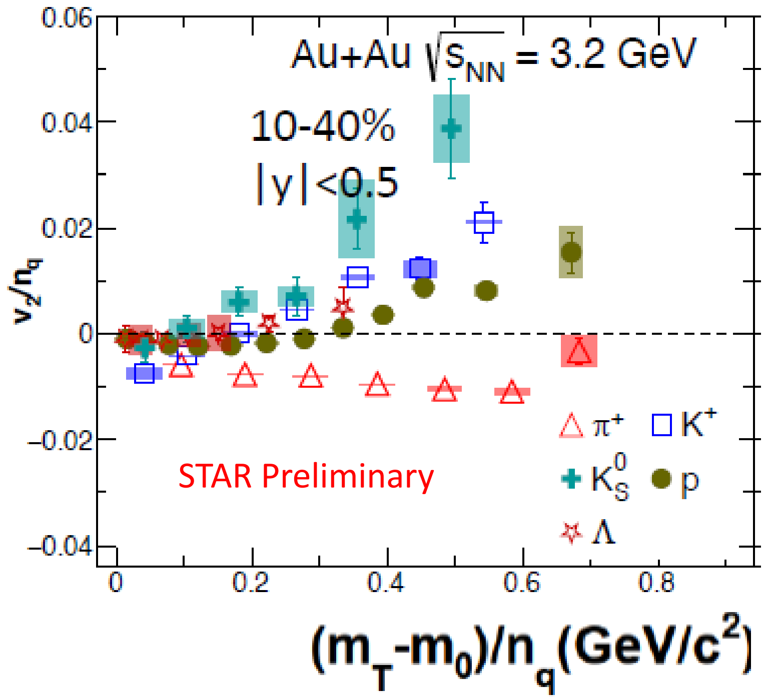

STAR Phys. Lett. B **827** (2022) 137003

Hypernuclei production

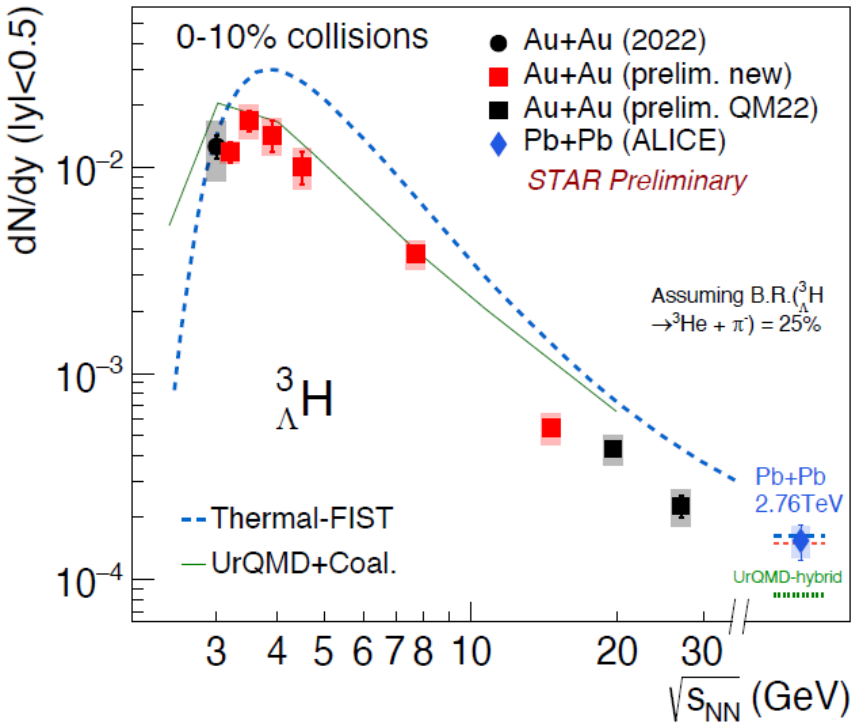

Coalescence calculation consistent with data at 3.5< $\sqrt{S_{NN}}$ <10 GeV, while still significantly higher than data at higher energies.

Thermal model fails to describe the trend at RHIC energies. Hypernuclei maybe dominantly produced after the hadron chemical freeze-out at RHIC.

The slopes of mid-rapidity v_1 for both light- and hyper-nuclei are scaled with A and/or mass across multiple collision energies

v_1 is consistent with hadronic transport (JAM2 mean field + coalescence)

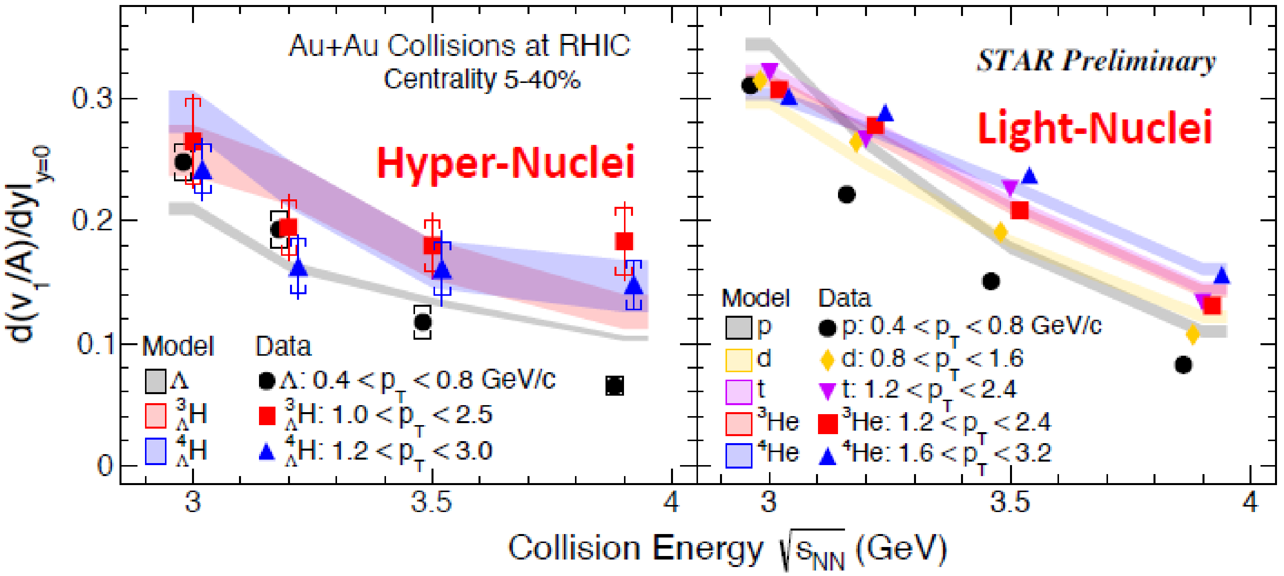

STAR Phys. Rev. Lett. **128,** 202301 (2022)
STAR Phys. Rev. Lett. **130**, 211301 (2023)

Two pion femtoscopy results from FXT program

$$C(q) = N[(1-\lambda) + \lambda K(q)(1+G(q))] \text{ , where}$$
$$G(q) = \exp(-q_{out}^2 R_{out}^2 - q_{side}^2 R_{side}^2 - q_{long}^2 R_{long}^2 - 2q_o q_l R_{ol}^2)$$

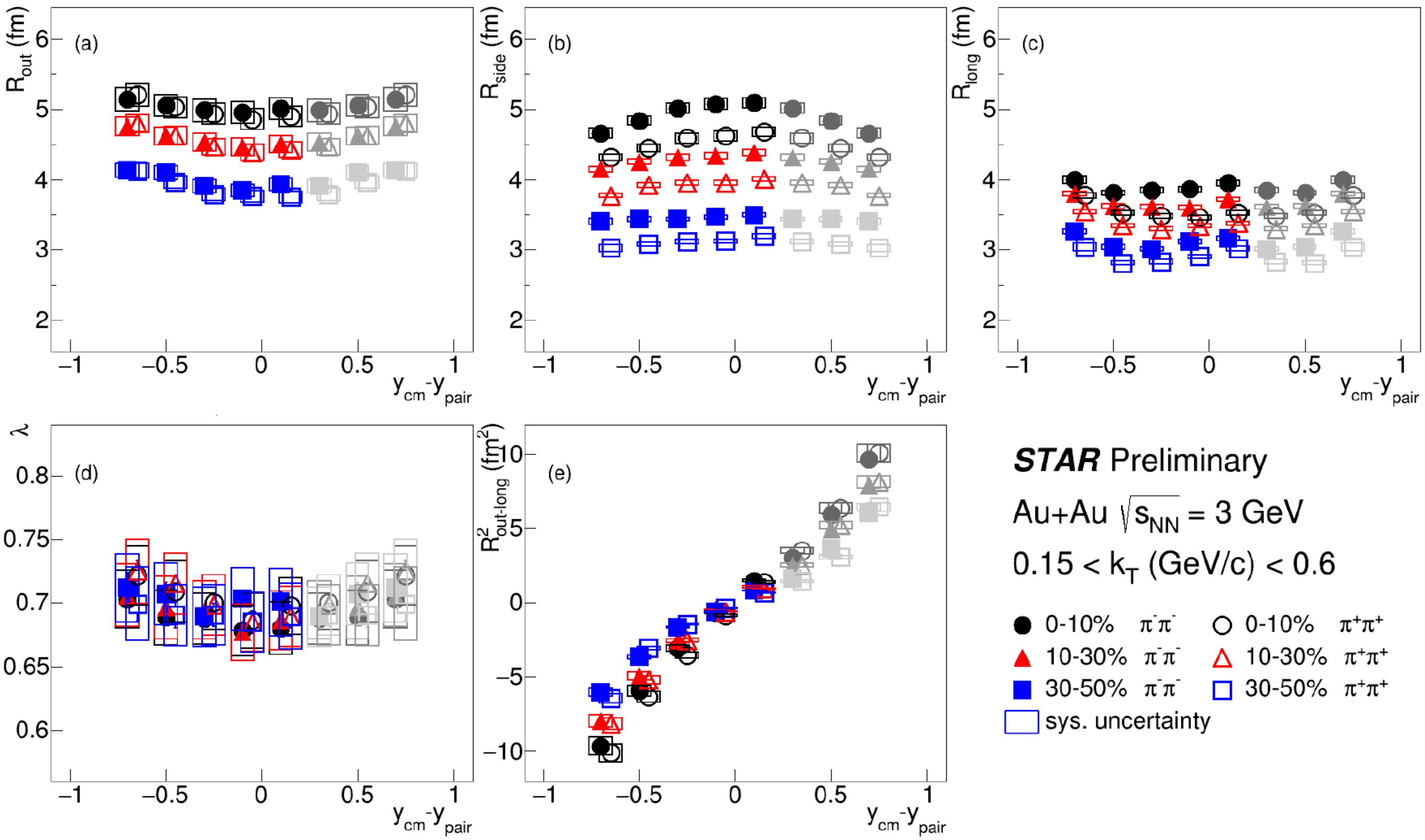

R_{side} decreases with going out of midrapidity:
➔ Hints on boost-invariance breaking

Clear rapidity dependence of $R^2_{out\text{-}long}$:
➔ Asymmetric rapidity window in analysis, could give rise to non-zero values in rapidity integrated measurement

R_{out}, R_{side} and R_{long} increase from peripheral to central collisions reflecting the geometry of the overlapping region.

Two pion femtoscopy results from FXT program

The source shape evolves from oblate to prolate, as energy increases

STAR. PRC 103, 034908(2021)

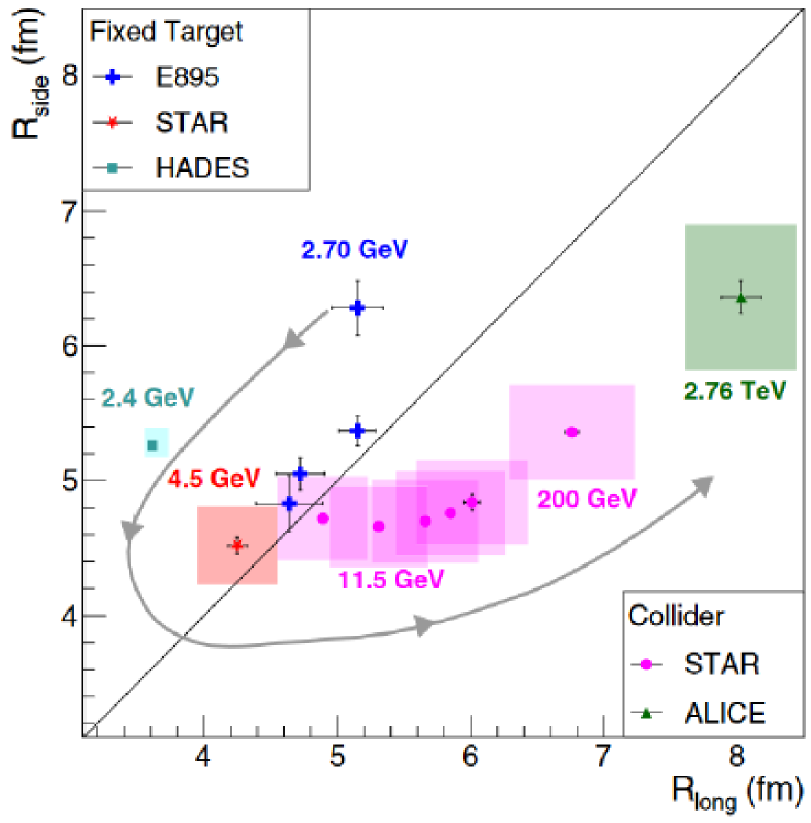

New results from the BES-II FXT on emittance volume is in better agreement with HADES results rather than AGS at low collision energies

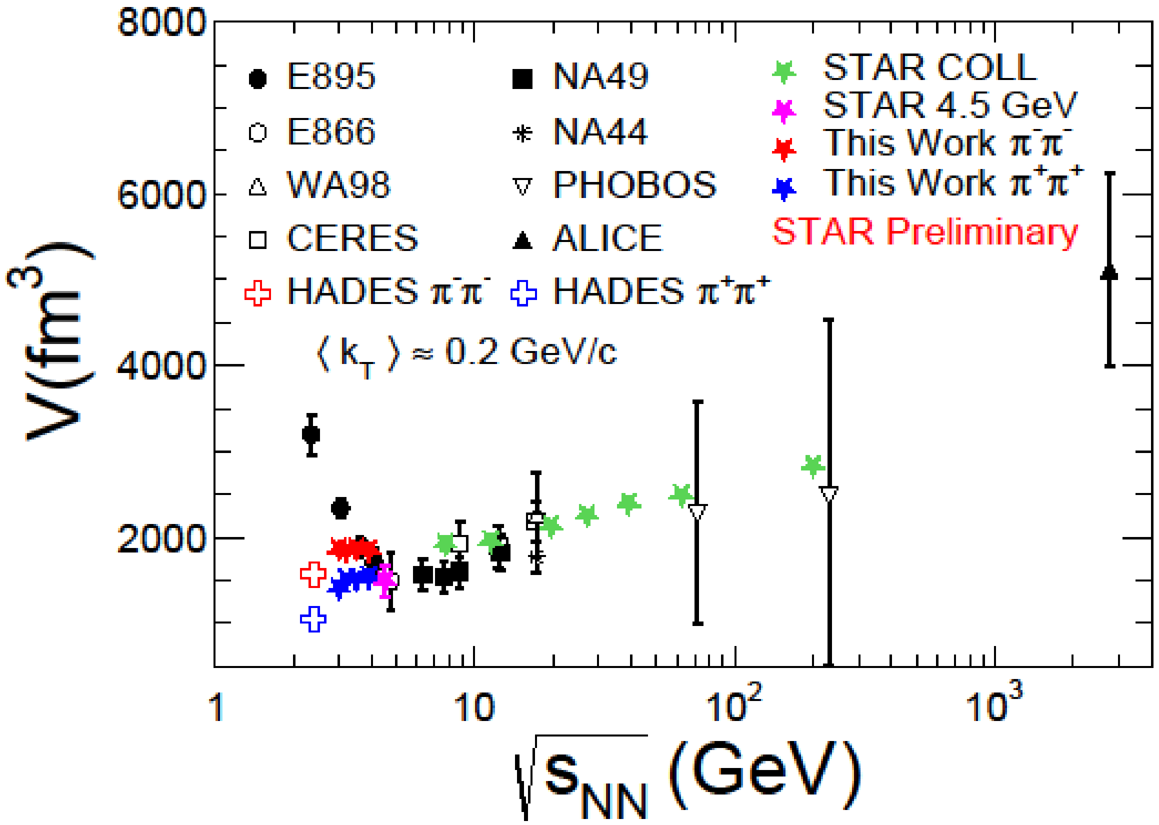

Top RHIC energy

Ω and φ production

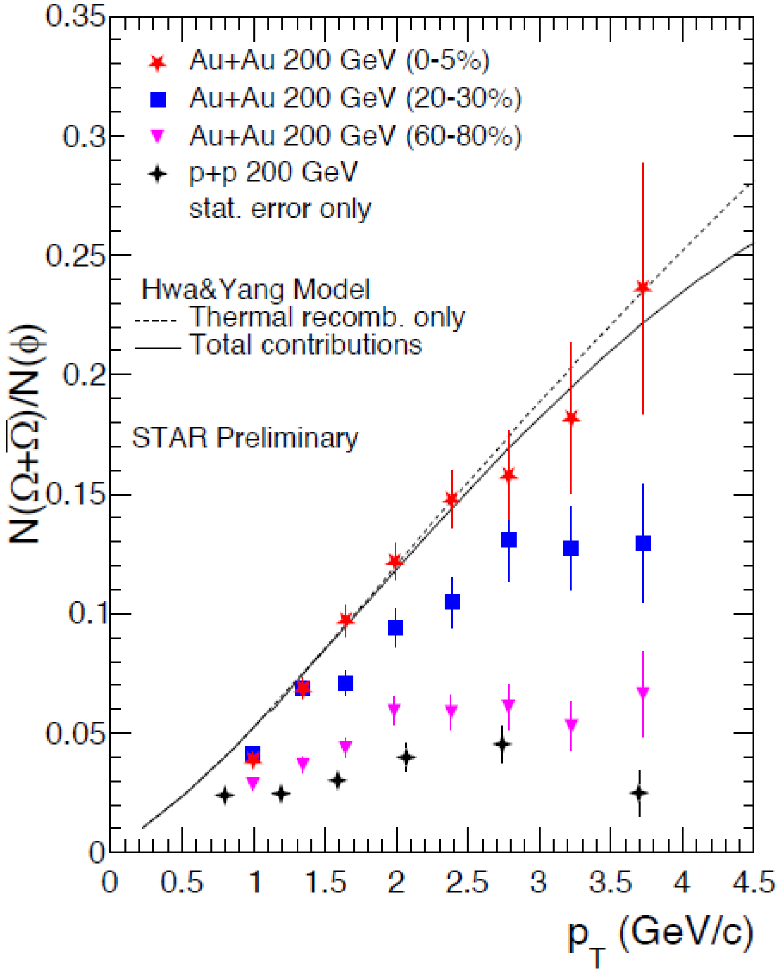

STAR Au+Au 200 GeV ϕ: Phys. Rev. Lett. 99(2007) 112301
STAR p+p 200 GeV Ω + $Ω: X. Zhu, QM2014;
STAR p+p 200GeV ϕ: STAR, Phys. Rev. C 79(2009) 064903
Theory: Phys. Rev. C, 2007, 75: 054904

Significant Ω enhancement over ϕ is observed in central AuAu collisions.

In central collisions, good agreement between data and recombination model calculations is obtained Ω and ϕ are predominantly produced through the recombination of thermalized strange quark in QGP.

Ω/ϕ ratio in p+p collisions is close to that in peripheral Au+Au collisions, hinting there may be smooth transition from p+p to Au+Au collisions.

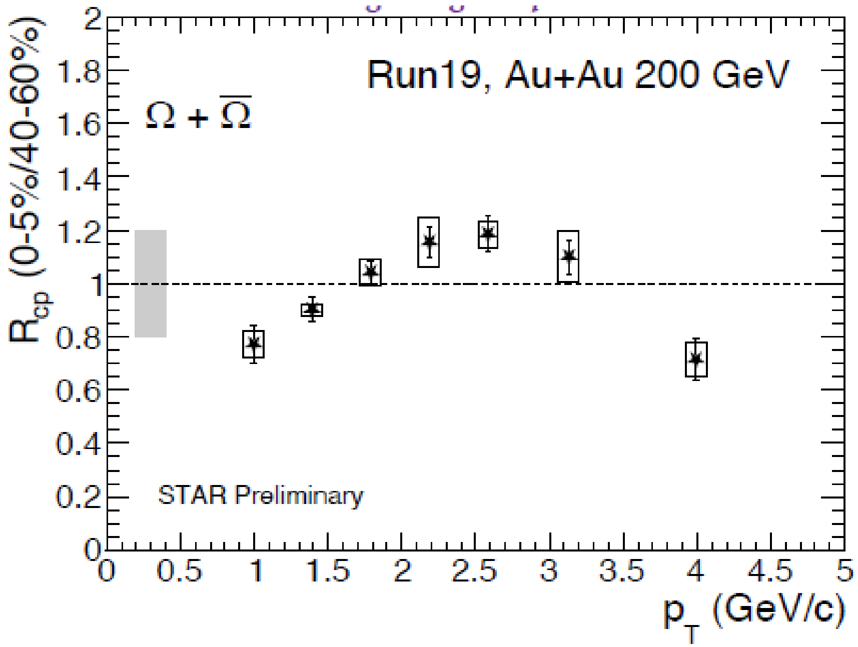

Measured R_{cp} hints the higher energy loss in dense nuclear matter, created at the most central collisions

Strange hadron production in small systems

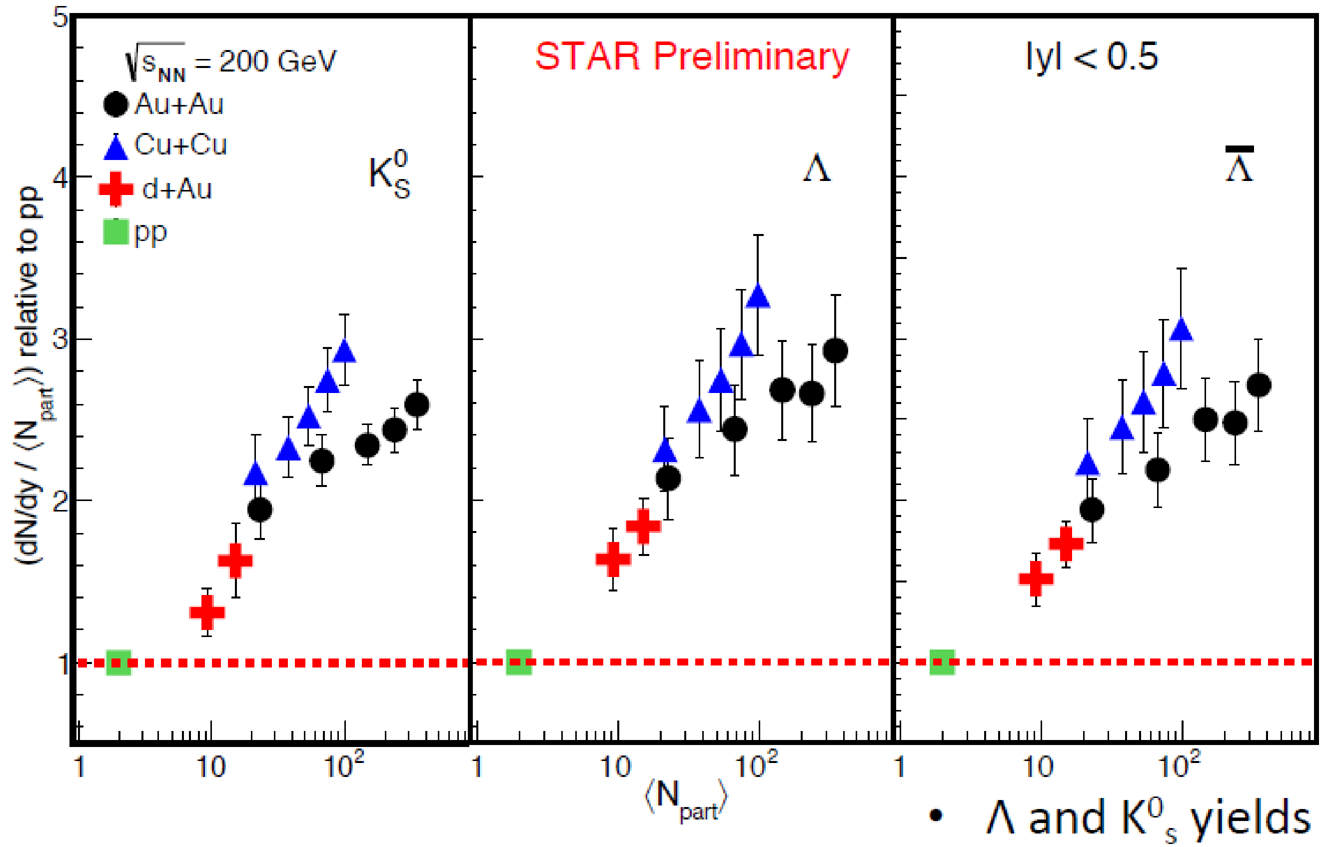

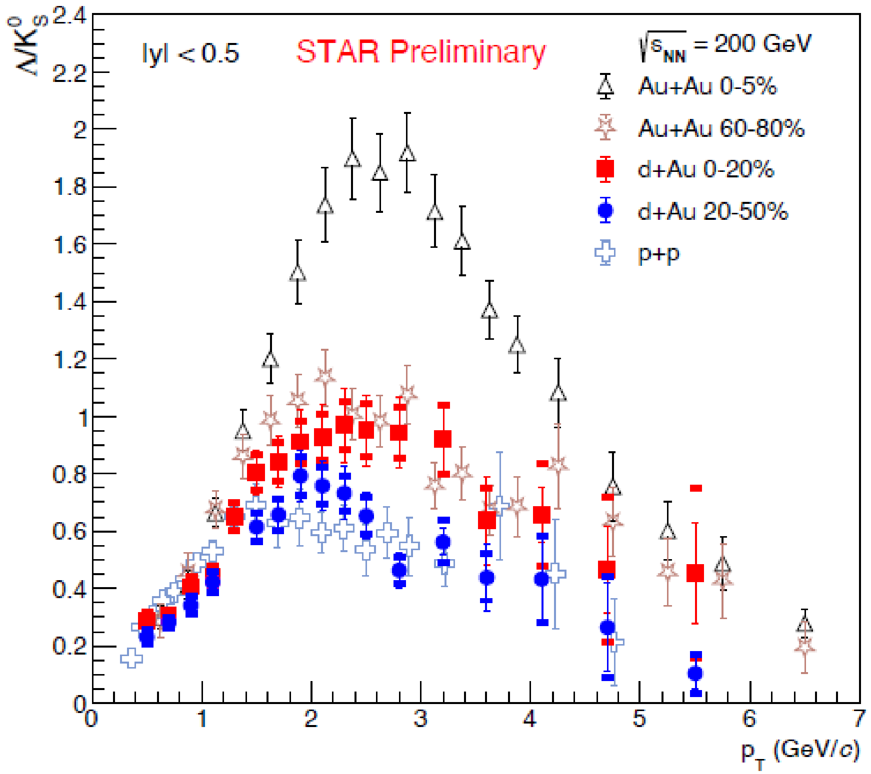

- Λ and K^0_s yields in d+Au at 200 GeV are enhanced

Baryon enhancement is observed at intermediate p_T for central d+Au 200 GeV with Λ/K^0_s

STAR : Phys. Rev. C **75**, 064901 (2007)
STAR : Phys. Rev. Lett. 108, 072301 (2012)
STAR : Phys. Rev. C **79**, 034909 (2009)

Flow in small systems

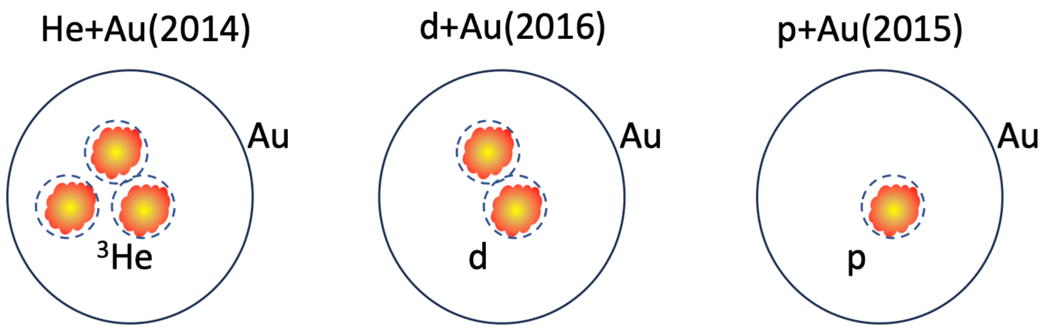

	Nucleon Glauber $\varepsilon_2(\varepsilon_3)$	Sub-Nucleon Glauber $\varepsilon_2(\varepsilon_3)$
0-5% pAu	0.23(0.16)	0.38(0.30)
0-5% dAu	0.54(0.18)	0.51(0.31)
0-5% ^{3}He+Au	0.50(0.28)	0.52(0.35)

Nucleon Glauber: J. L. Nagle, et. al., PRL 113 (2014) 112301
Sub-nucleon: K. Welsh, et. al., PRC 94 (2016) 024919

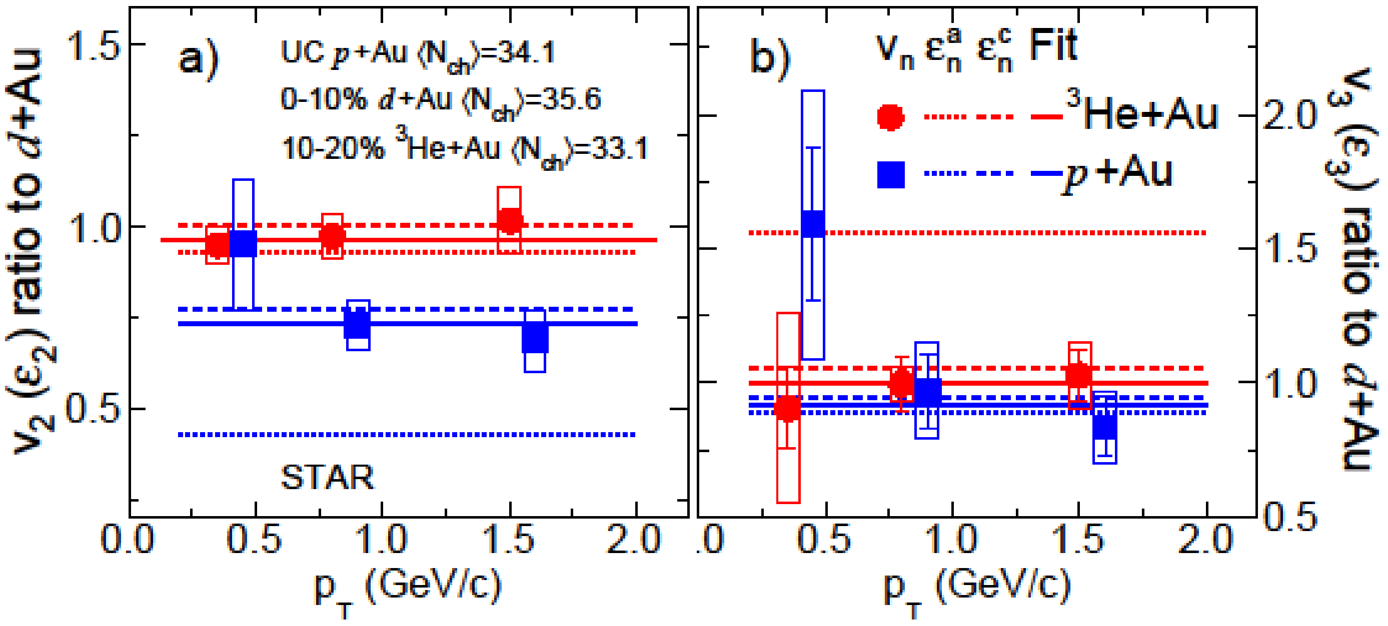

- Data at midrapidity
  - $v_2^{\text{He+Au}} \sim v_2^{\text{d+Au}} > v_2^{\text{p+Au}}$
  - $v_3^{\text{He+Au}} \sim v_3^{\text{d+Au}} \sim v_3^{\text{p+Au}}$
- Suggests significant influence of sub-nucleonic fluctuations
  - Need to study pre-flow

STAR, PRL 130 (2023) 242301

Hadron production in jets

p+p vs. Au+Au

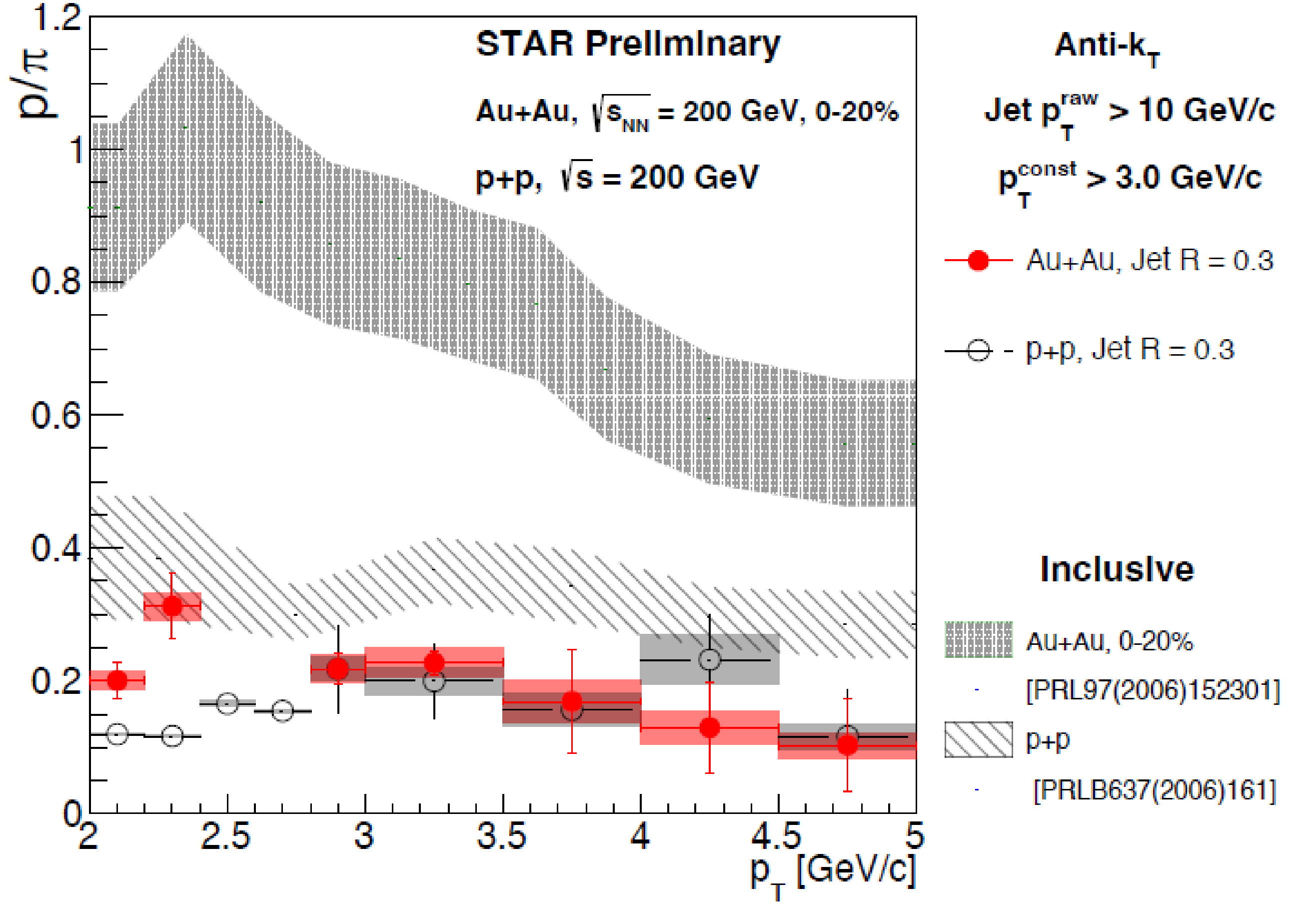

- *p*/*π* ratio significantly smaller in jets compared to bulk
- Similar *p*/*π* ratio in jets with p_T^{const} > 3 GeV/c in *p*+*p* and Au+Au collisions
- Measurements with lower p_T^{const} cuts are underway

Light nuclei production in isobar collisions

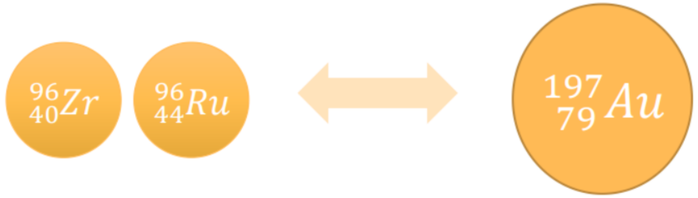

Yields and mean p_T as a function of collision multiplicity

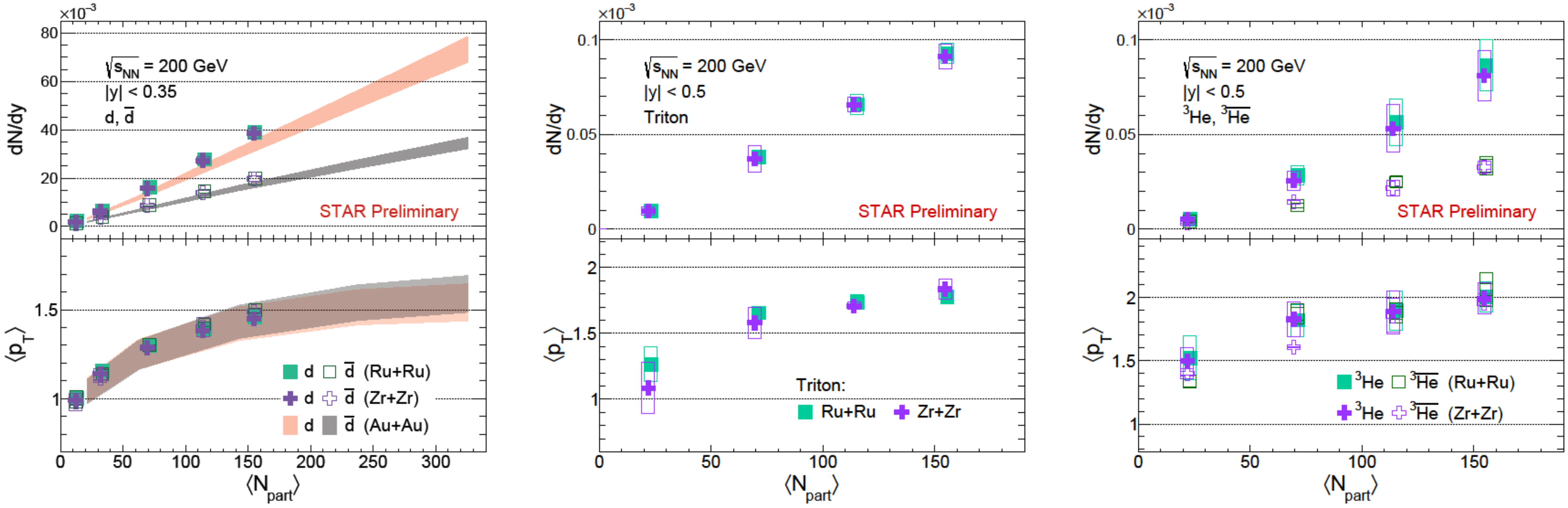

Yields and mean p_T of deuterons and anti deuterons in Ru+Ru and Zr+Zr collisions agree well with Au+Au collisions within the uncertainty

Heavy flavor production at STAR

$$R_{AA} = \frac{1}{N_{coll}} \times \frac{dN^2_{AA}/(dp_T dy)}{dN^2_{pp}/(dp_T dy)}$$

For the J/Ψ:
Low p_T: significant CNM effects. Consistent with model predictions
High p_T (> 3 GeV/c): R_{pAu} consistent with unity → suppression in AA due to QGP effects

STAR, Phys. Lett. B 797 (2019) 134917
STAR, Phys. Lett. B 825 (2022) 136865

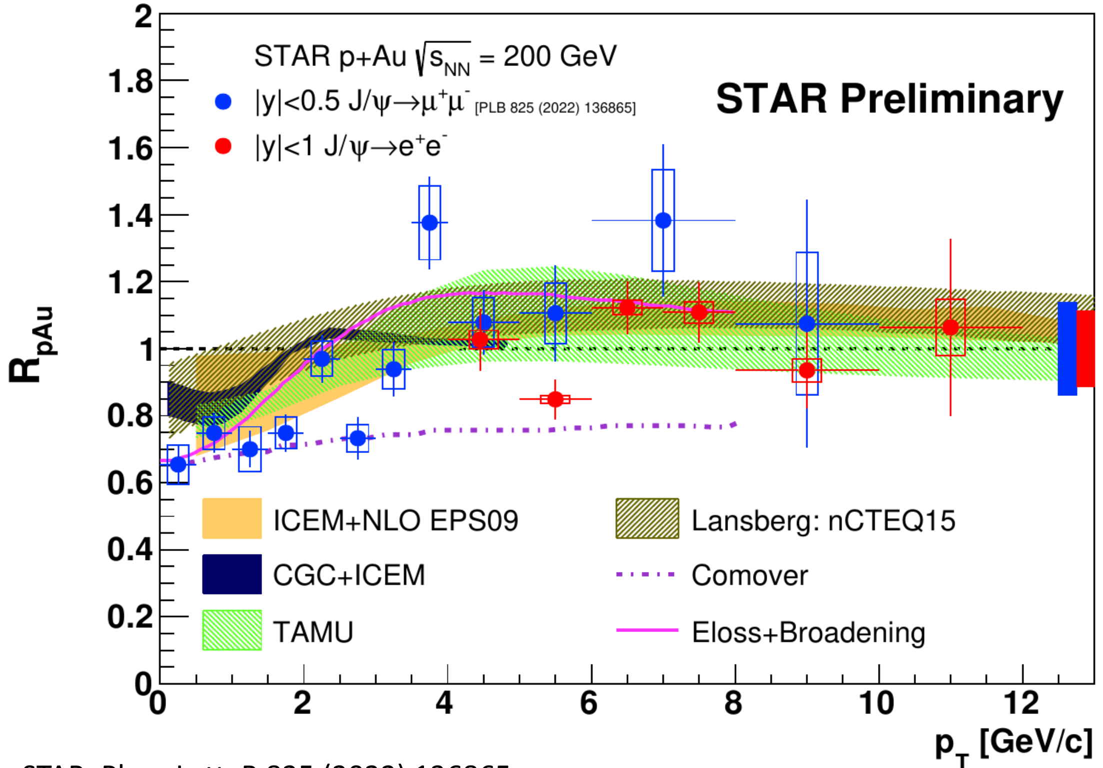

STAR, Phys. Lett. B 825 (2022) 136865

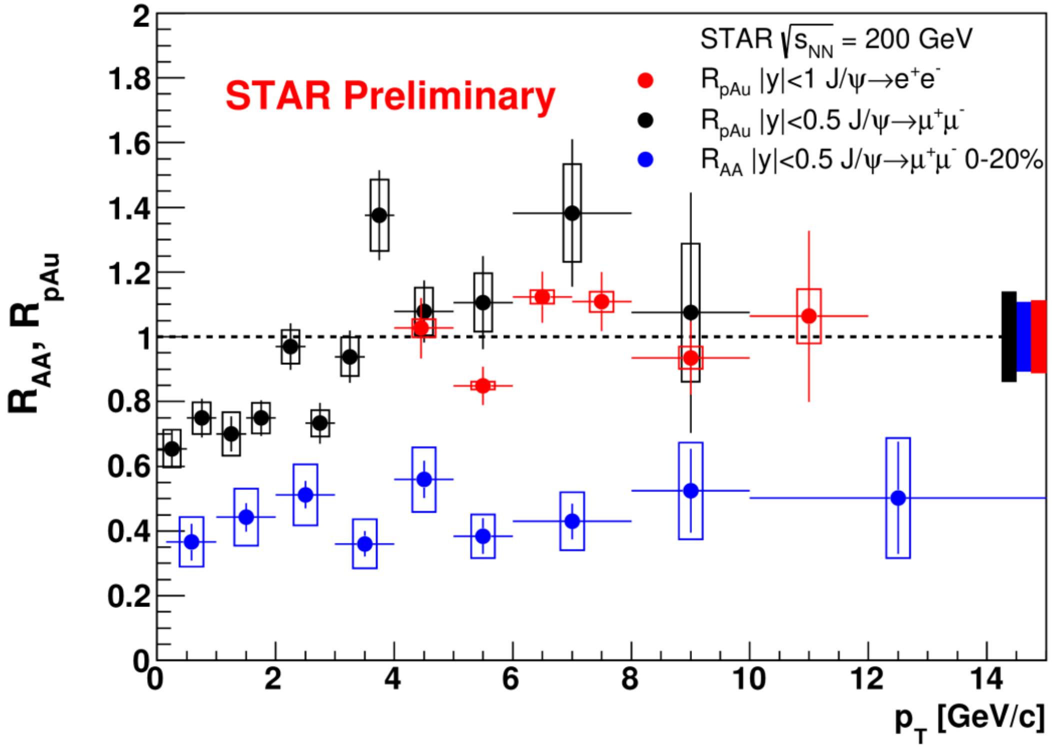

Heavy flavor production at STAR

- Significant suppression of different Υ states in Au+Au collisions at 200 GeV
- Similar R_{AA} for Υ states in isobar collisions as in Au+Au at 200 GeV
- No significant collision species dependence of the suppression at similar $\langle N_{part} \rangle$ for the J/Ψ

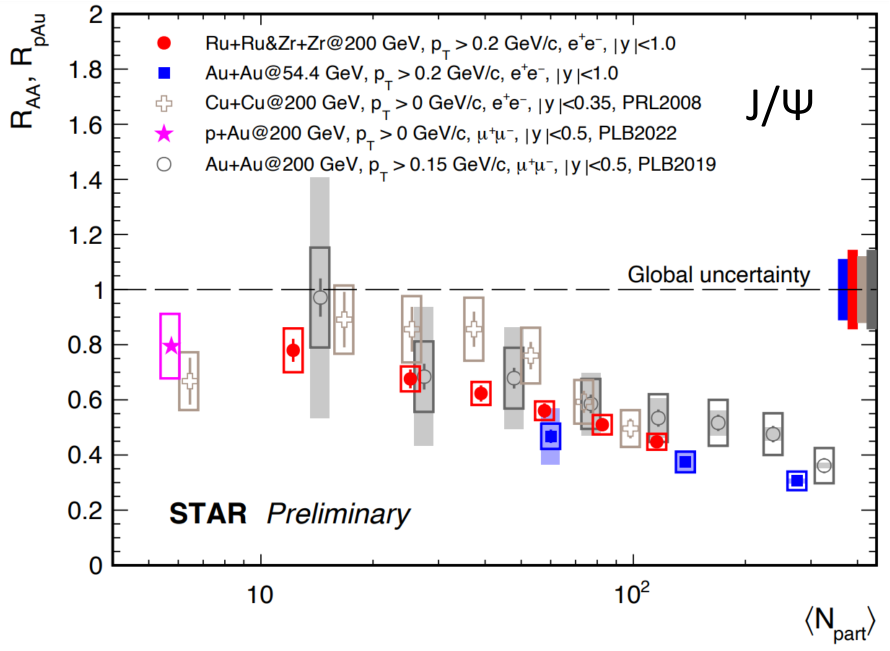

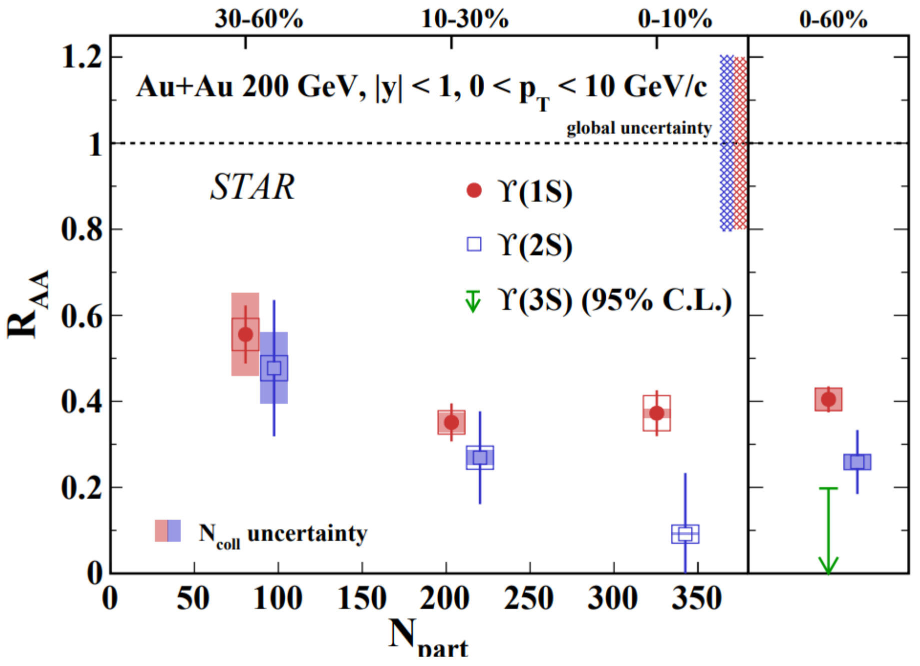

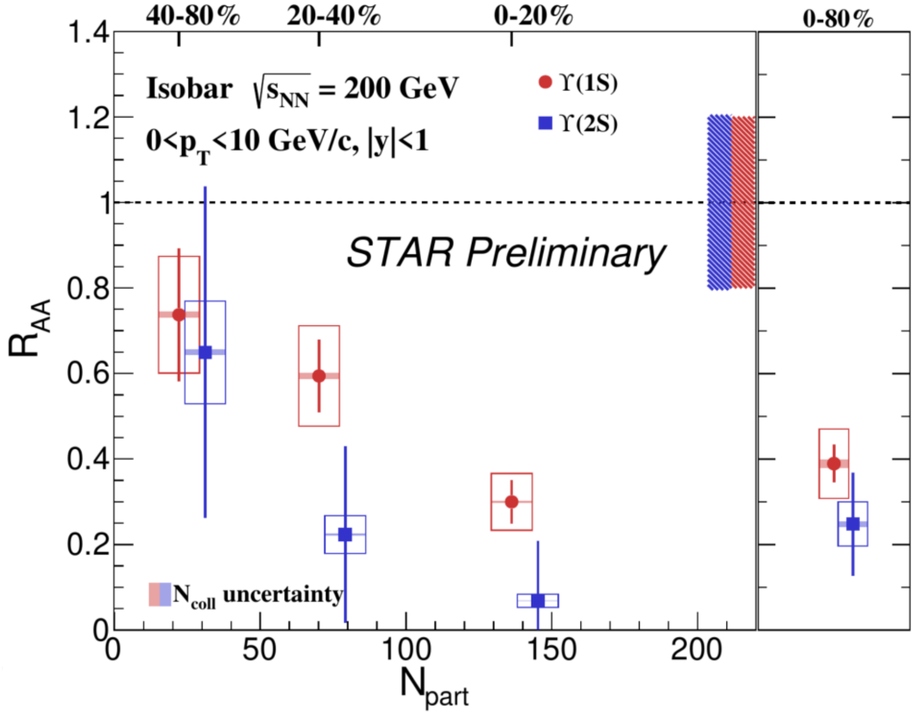

STAR, Phys. Lett. B 797 (2019) 134917
STAR, Phys. Lett. B 825 (2022) 136865
STAR, Phys. Rev. Lett. 130 (2023) 112301

Cold QCD effects

Gluon polarization impact on proton spin

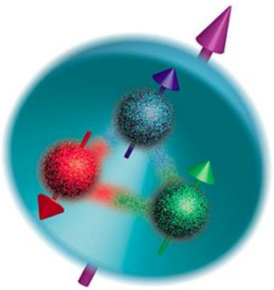

$$S = \frac{1}{2} = \frac{1}{2}\Delta\Sigma + \Delta G + L$$

quarks — gluons — orbital angular momentum

DSSV global fit including up-to-date jet, dijet, pion, W data

DSSV14 + RHIC (≤2022):

- $\Delta G = \int_{0.05}^{1} \Delta g(x)dx = 0.22 \pm 0.03$
- $\Delta G = \int_{0.001}^{0.05} \Delta g(x)dx = 0.17 \pm 0.20$

DSSV14:

- $\Delta G = \int_{0.05}^{1} \Delta g(x)dx = 0.20 \pm 0.06$
- $\Delta G = \int_{0.001}^{0.05} \Delta g(x)dx = 0.15 \pm 0.50$

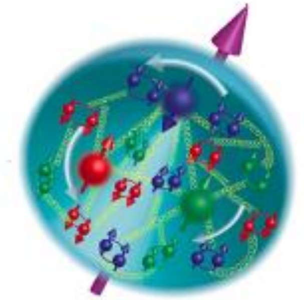

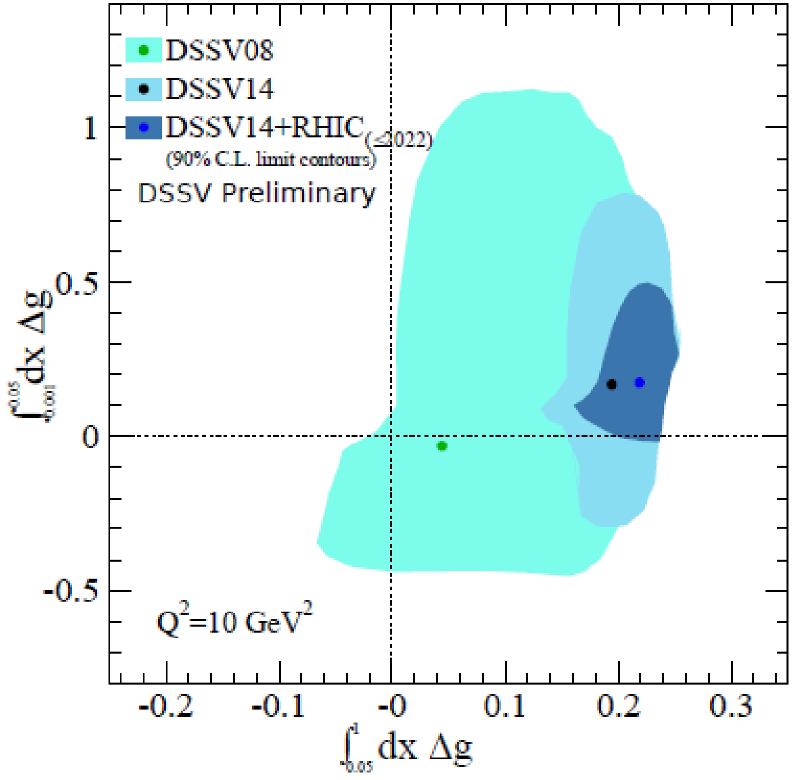

arXiv:2302.00605

Single spin asymmetry

W bosons production sensitive to flavor, spin, charge simultaneously
Powerful tool to probe sea quark polarization

First experimental observation of a flavor-asymmetry between anti-up and anti-down polarizations, opposite to the unpolarized distributions

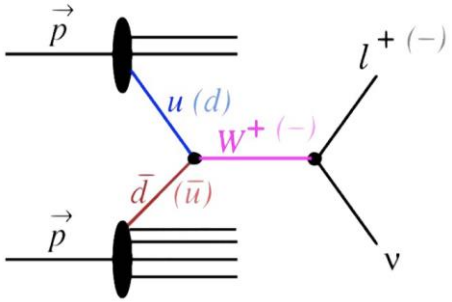

$$A_L = \frac{\sigma^+ - \sigma^-}{\sigma^+ + \sigma^-}$$

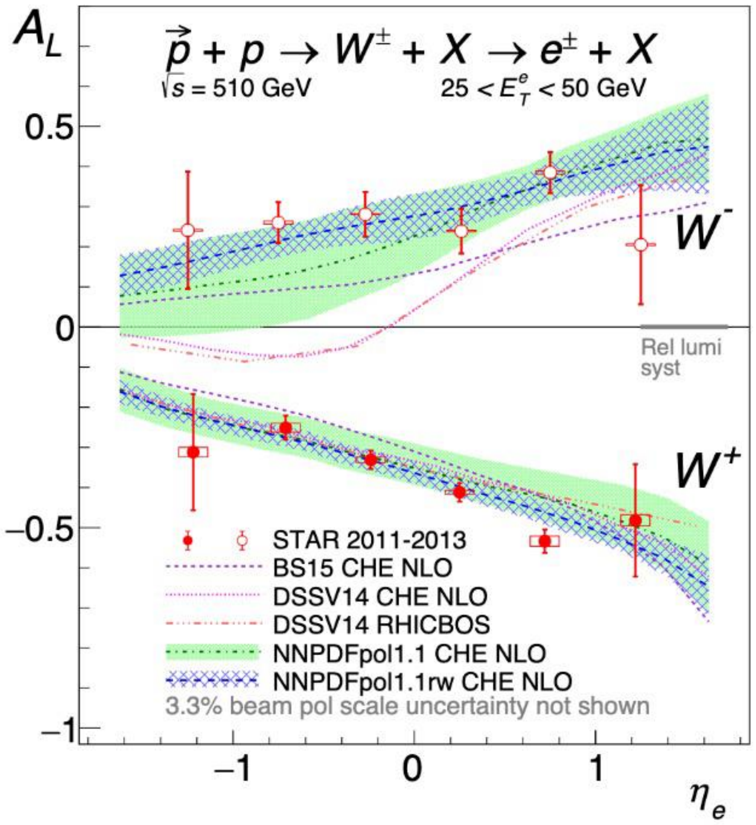

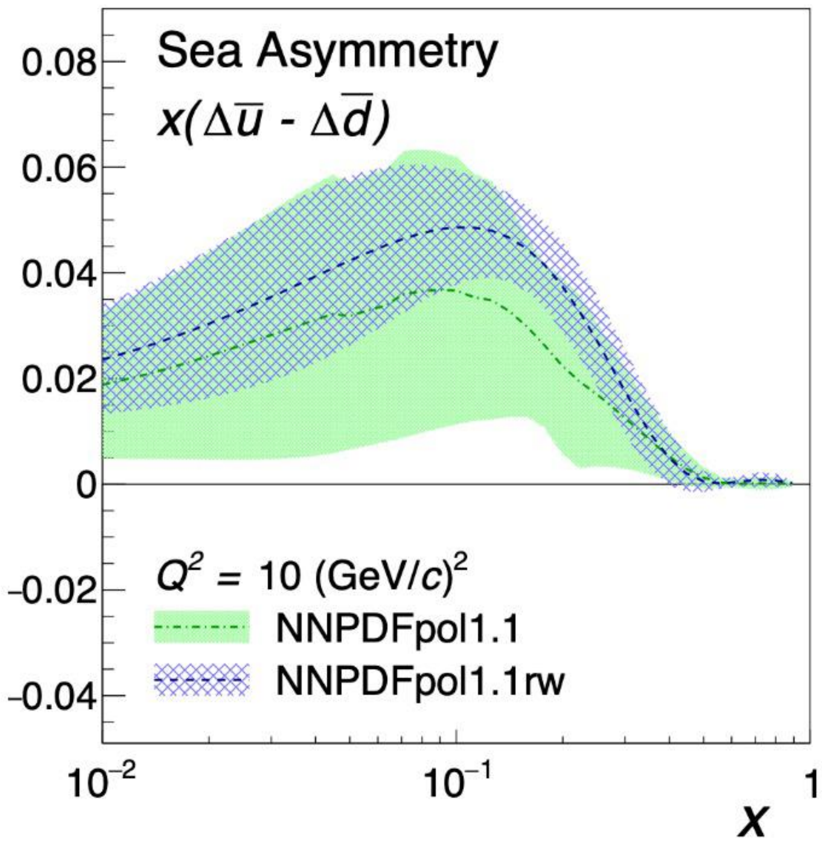

STAR, PRD 99, 051102(R) (2019)

Double spin asymmetry

Di-jet measurements

Sub-processes directly sensitive to gluon
Constrain gluon helicity-dependent PDFs

$$A_{LL} = \frac{\sigma^{\uparrow\uparrow} - \sigma^{\uparrow\downarrow}}{\sigma^{\uparrow\uparrow} + \sigma^{\uparrow\downarrow}} \propto \overbrace{\frac{\Delta f_1}{f_1} \otimes \frac{\Delta f_2}{f_2}}^{\text{probed}} \otimes \overbrace{\hat{a}_{LL} \otimes D_f^h}^{\text{inputs}}$$

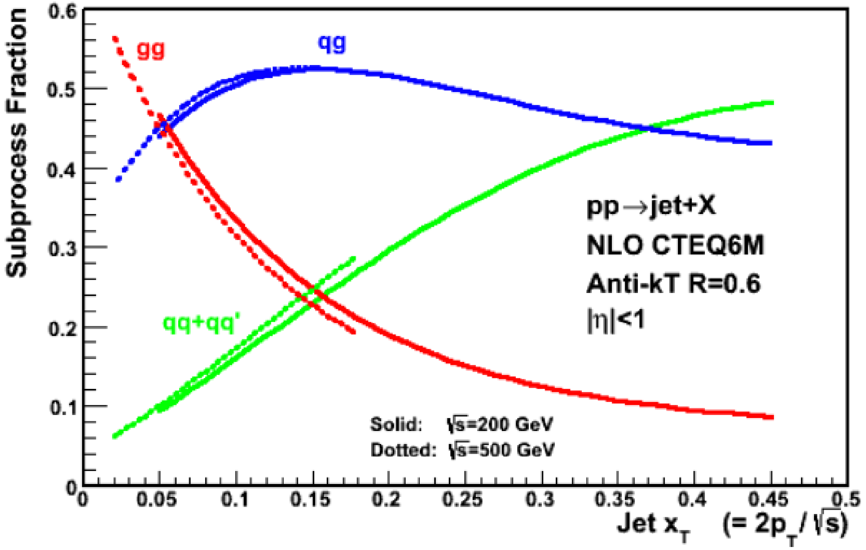

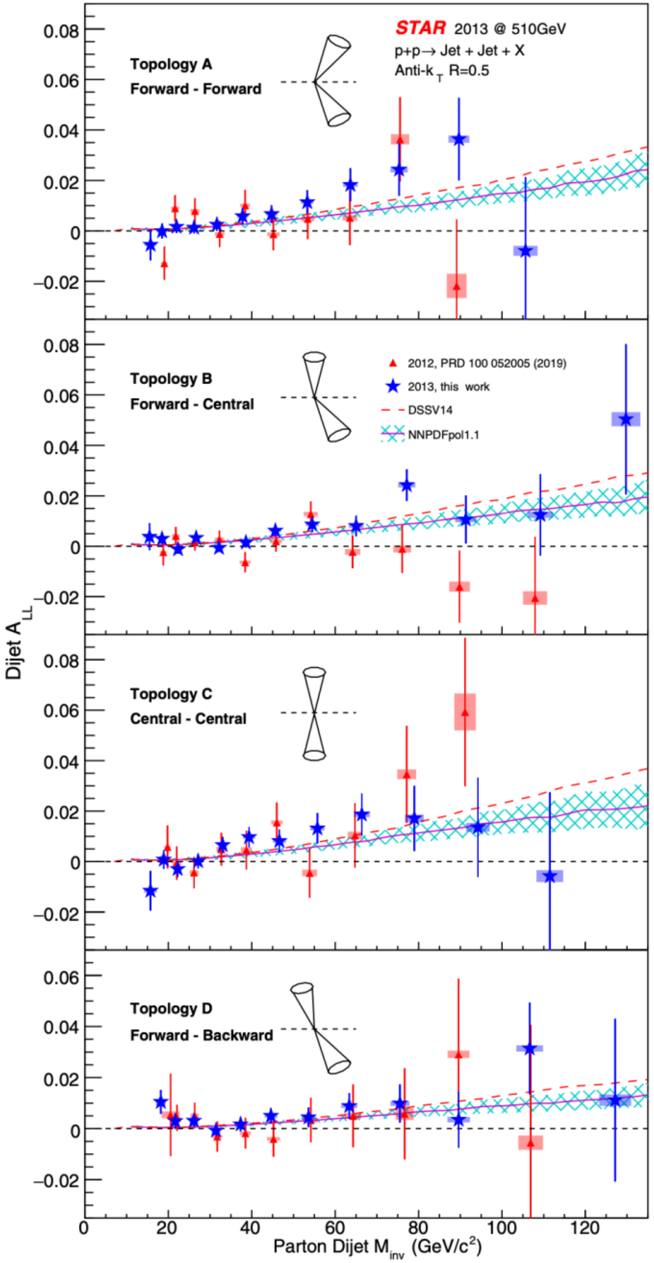

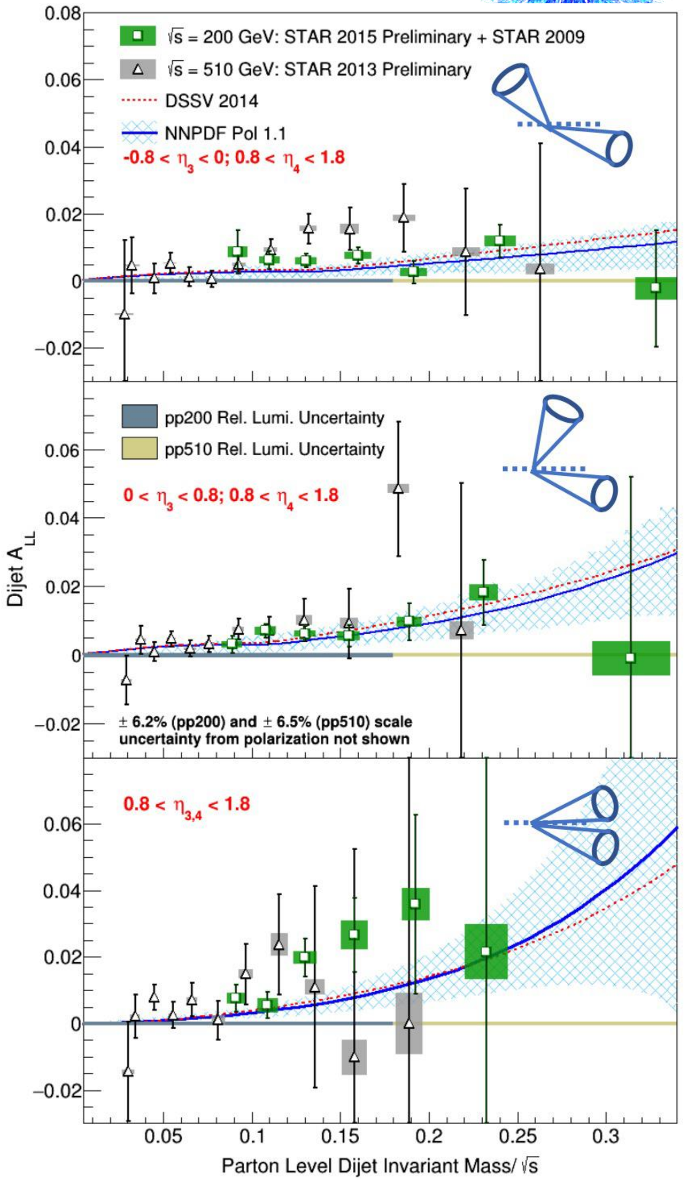

STAR Phys. Rev. D 105, 092011 (2022)
STAR Phys. Rev. D 103, L091103 (2021)

Measurements with unpolarized beam

$\bar{d}/\bar{u}$ with $W^{\pm}$ cross section ratio

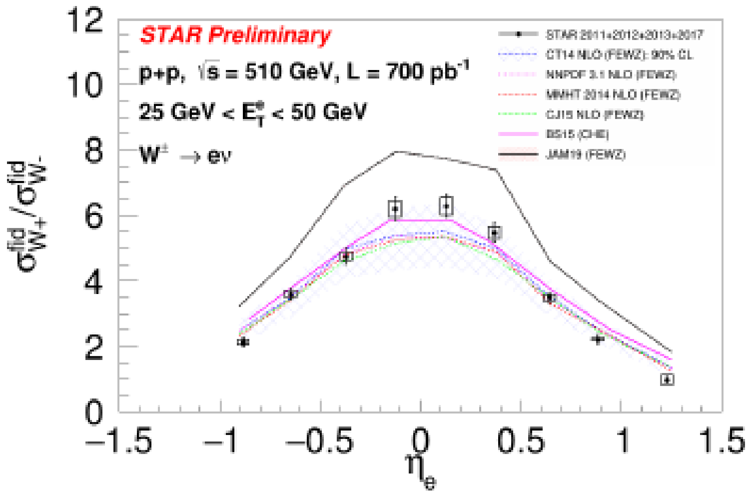

Differential Z^0 cross section

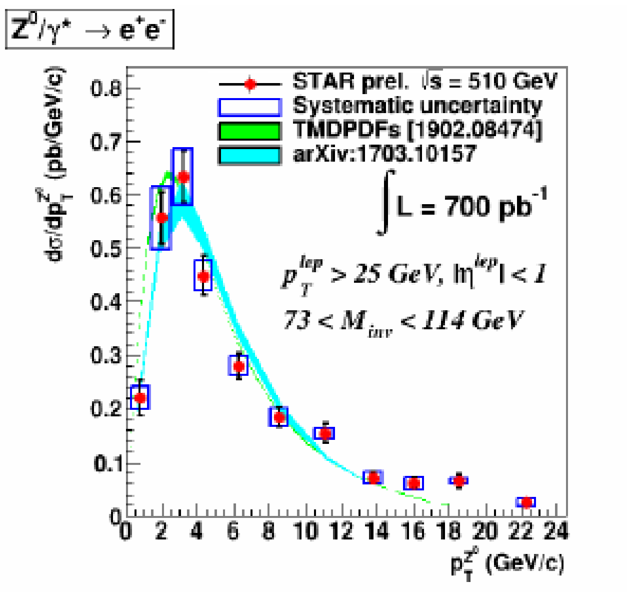

Gluon PDF with Jet cross section

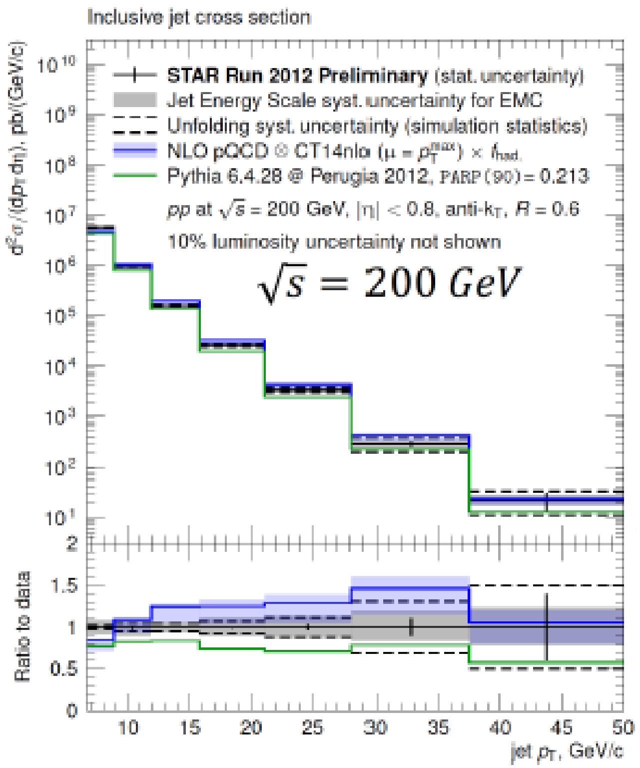

Successful STAR run 2022 with forward upgrade

Requested luminosity for the last transverse spin run in 2024 before EIC

$\sqrt{s}$ (GeV)	Species	Luminosity	Year
508	$\mathrm{p}^{\uparrow} + \mathrm{p}^{\uparrow}$	400 pb^{-1}	2022
200	$\mathrm{p}^{\uparrow} + \mathrm{p}^{\uparrow}$	235 pb^{-1}	2024
200	$\mathrm{p}^{\uparrow} + \mathrm{Au}$	1.3 pb^{-1}	2024

And much more to come with STAR detector upgrades and high statistics runs 2023-2025

Summary

- ✓ STAR experimental program covers a wide range of topics and STAR has collected a unique set of data on a variety of collision systems and collision energies including fixed target data

- ✓ STAR detector has gone through several upgrades in a last couple of years to extend it’s capabilities for high statistics runs

- ✓ BES-II has increased statistics by a factor of 10 for most of the energies and provided additional data with FXT mode of STAR detector

- ✓ Run 23 was the 1-st top energy Au+Au with all upgrades. STAR recorded 6.5B events before unexpected RHIC shutdown

- ✓ Data taking has been very successfully ongoing and new results are on the way with our future high statistics Au+Au/p+p/p+Au runs

Thank you for the attention!

Part of this work was supported by Russian Science Foundation under grant № 22-72-10028

Backup slides

BES-II statistics and run time

Recent BES-II, FXT and 200 GeV datasets (years 2018-2021)

$\sqrt{s_{NN}}$ (GeV)	Beam Energy (GeV/nucleon)	Collider or Fixed Target	$y_{center\ of\ mass}$	μ_B (MeV)	Run Time (days)	No. Events Collected (Request)	Date Collected
200	100	C	0	25	2.0	138 M (140 M)	Run-19
27	13.5	C	0	156	24	555 M (700 M)	Run-18
19.6	9.8	C	0	206	36	582 M (400 M)	Run-19
17.3	8.65	C	0	230	14	256 M (250 M)	Run-21
14.6	7.3	C	0	262	60	324 M (310 M)	Run-19
13.7	100	FXT	2.69	276	0.5	52 M (50 M)	Run-21
11.5	5.75	C	0	316	54	235 M (230 M)	Run-20
11.5	70	FXT	2.51	316	0.5	50 M (50 M)	Run-21
9.2	4.59	C	0	372	102	162 M (160 M)	Run-20+20b
9.2	44.5	FXT	2.28	372	0.5	50 M (50 M)	Run-21
7.7	3.85	C	0	420	90	100 M (100 M)	Run-21
7.7	31.2	FXT	2.10	420	0.5+1.0+ scattered	50 M + 112 M + 100 M (100 M)	Run-19+20+21
7.2	26.5	FXT	2.02	443	2+Parasitic with CEC	155 M + 317 M	Run-18+20
6.2	19.5	FXT	1.87	487	1.4	118 M (100 M)	Run-20
5.2	13.5	FXT	1.68	541	1.0	103 M (100 M)	Run-20
4.5	9.8	FXT	1.52	589	0.9	108 M (100 M)	Run-20
3.9	7.3	FXT	1.37	633	1.1	117 M (100 M)	Run-20
3.5	5.75	FXT	1.25	666	0.9	116 M (100 M)	Run-20
3.2	4.59	FXT	1.13	699	2.0	200 M (200 M)	Run-19
3.0	3.85	FXT	1.05	721	4.6	259 M -> 2B(100 M -> 2B)	Run-18+21

BES-I (years 2010, 2011, 2014)

$\sqrt{s_{NN}}$ (GeV)	No. of events (million)
7.7	4
11.5	8
19.6	17.3
27	33
39	111

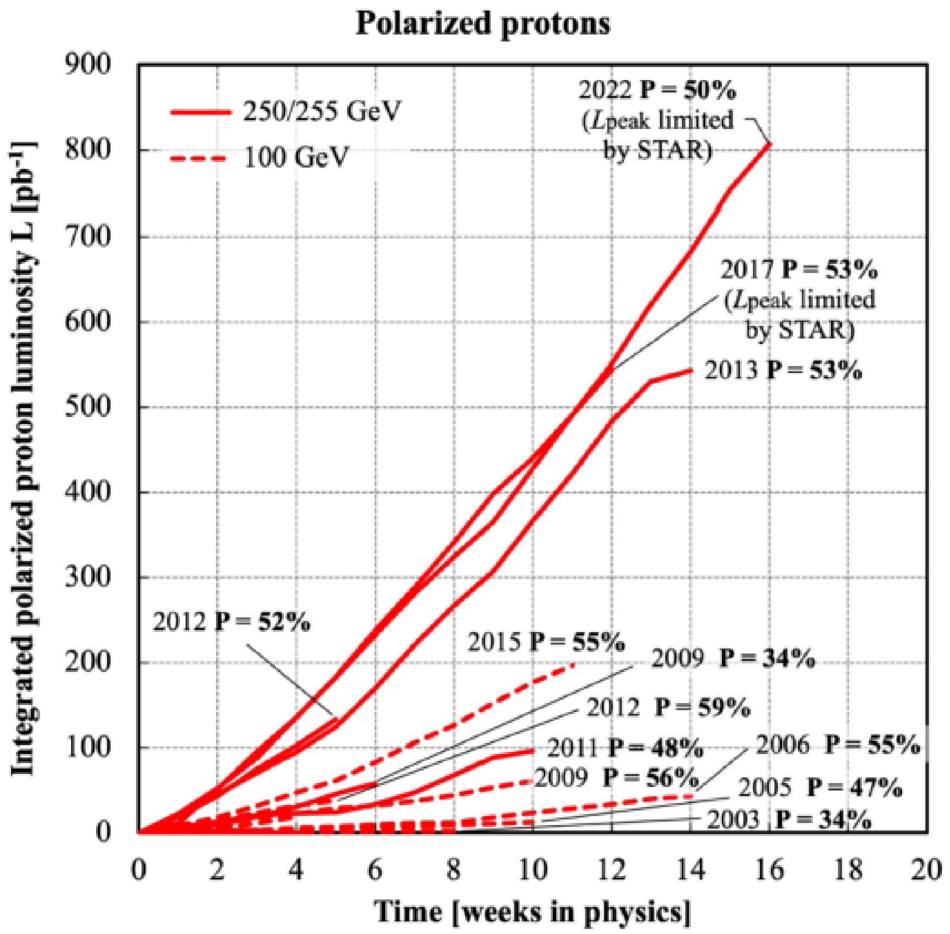

	Year	√s (GeV)	L (pb^{-1})	<P> (%)
Long.	2006	62.4	--	48
		200	6.8	57
	2009	200	25	38
		500	10	55
	2011	500	12	48
	2012	510	82	56
	2013	510	256	56
	2015	200	50	60
Trans.	2006	62.4	0.2	48
		200	8.5	57
	2008	200	7.8	45
	2011	500	25	55
	2012	200	22	60
	2015	200	50	60
	2017	510	356	55
	2022	508	400	50

STAR

Particle identification at 3 GeV

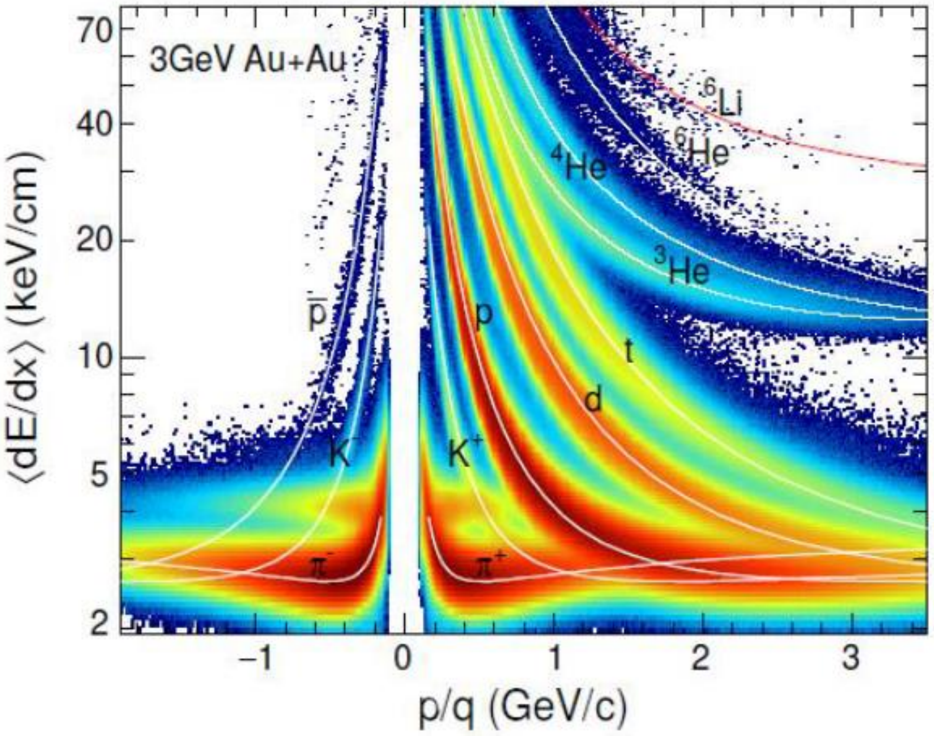

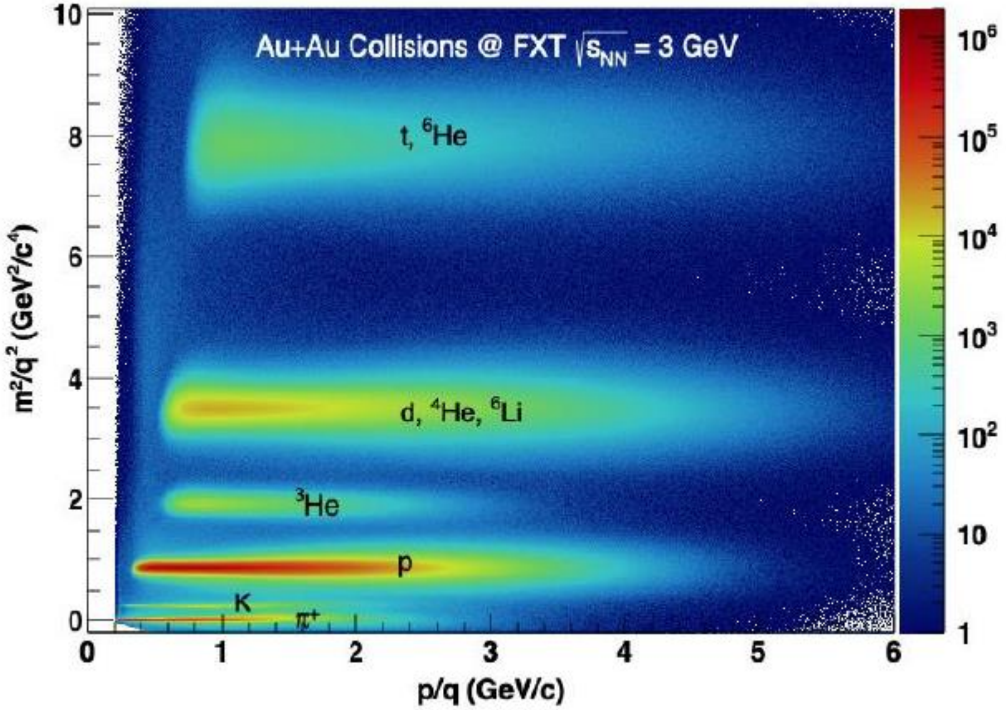

Detects particles in the $0 < \eta < 2$ range
π, K, p, d, t, h, α through dE/dx and ToF
K^0_s, Λ, Ξ, Ω, φ, $^3_\Lambda H$, $^4_\Lambda H$ trough invariant mass

About 260M events analyzed from 2018,
2B more recorded in 2021

Hypernuclei production

300M Au+Au data without iTPC and eTOF

Candidate reconstruction via invariant mass in two body decay

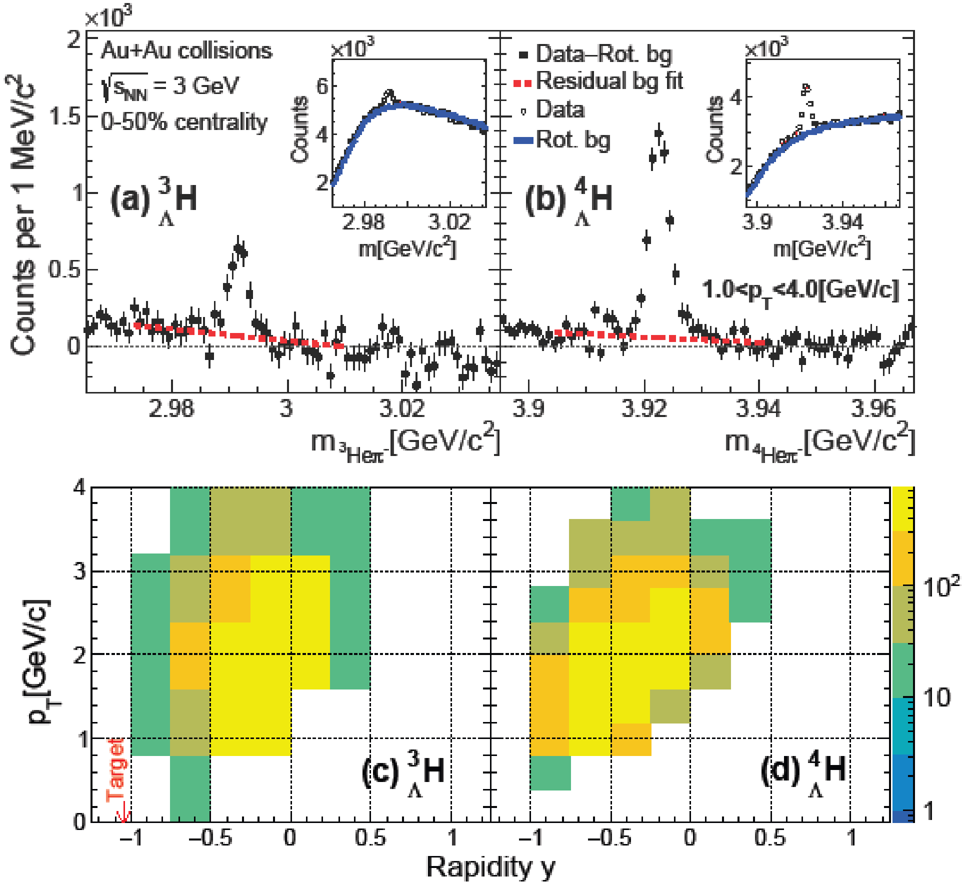

$$^{3}_{\Lambda}H \rightarrow {}^{3}He + \pi^{-}$$

$$^{4}_{\Lambda}H \rightarrow {}^{4}He + \pi^{-}$$

Measured lifetime results at $\sqrt{s_{NN}}$ = 3.0 and 7.2 GeV are in a good agreement with each other

The combined results are

$$\tau({}^{3}_{\Lambda}H) = 221 \pm 15(stat.) \pm 19(syst.)\ ps.$$

$$\tau({}^{4}_{\Lambda}H) = 218 \pm 6(stat.) \pm 13(syst.)\ ps.$$

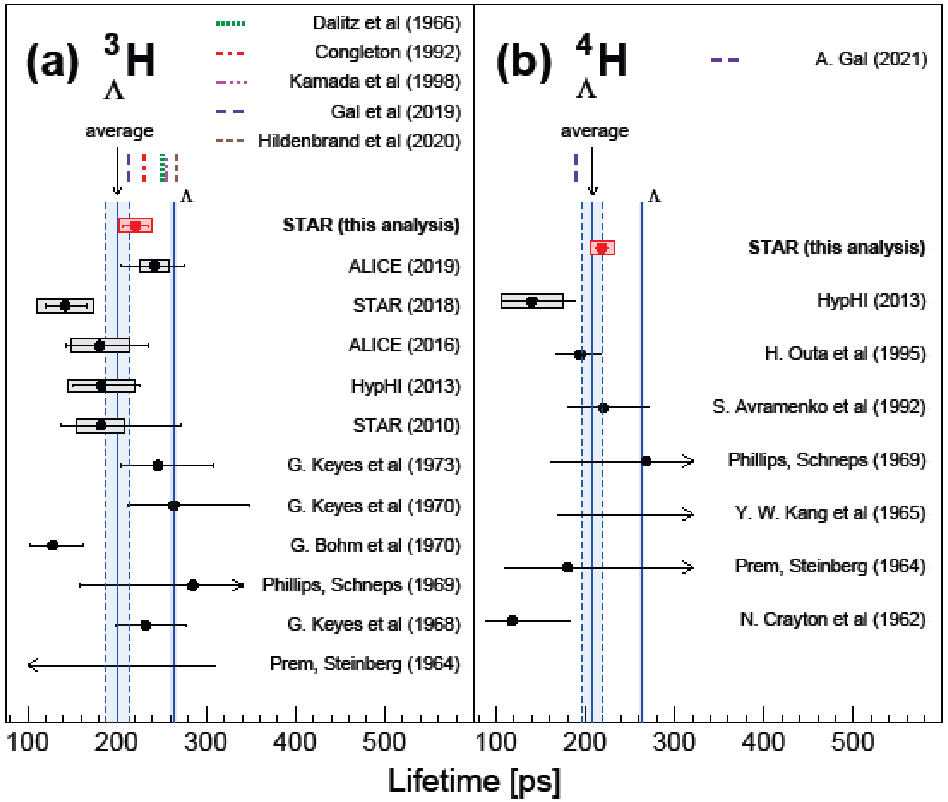

Lifetime measurements are consistent with previous measurements and have higher precision

PRL **128** (2022) 202301

Global hyperon polarization measurements

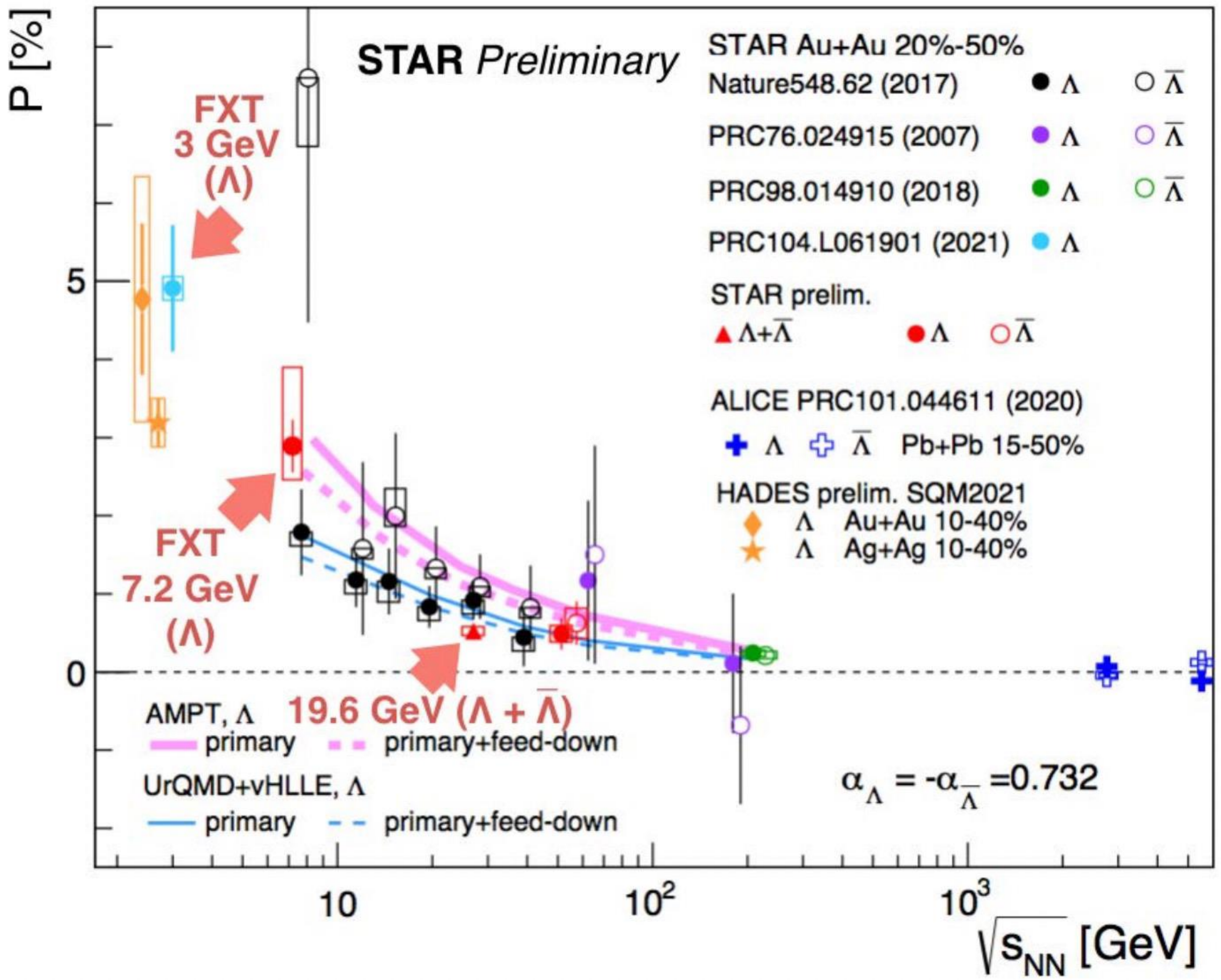

Global hyperon polarization over a large range of collision energy is measured and can be described by hydrodynamic and transport models with intense fluid vorticity of the QGP

The observation of substantial polarization in these collisions may require a reexamination of the viscosity of any fluid created in the collision, of the thermalization timescale of rotational modes, and of hadronic mechanisms to produce global polarization.

$$\frac{dN}{d\cos\theta^*} = \frac{1}{2}\left(1 + \alpha_H |\vec{\mathcal{P}}_H| \cos\theta^*\right)$$

Nature 548 (2017) 62,
PRC **104** (2021) 061901,
arXiv: 2204.02302

Collectivity and temperature of the medium

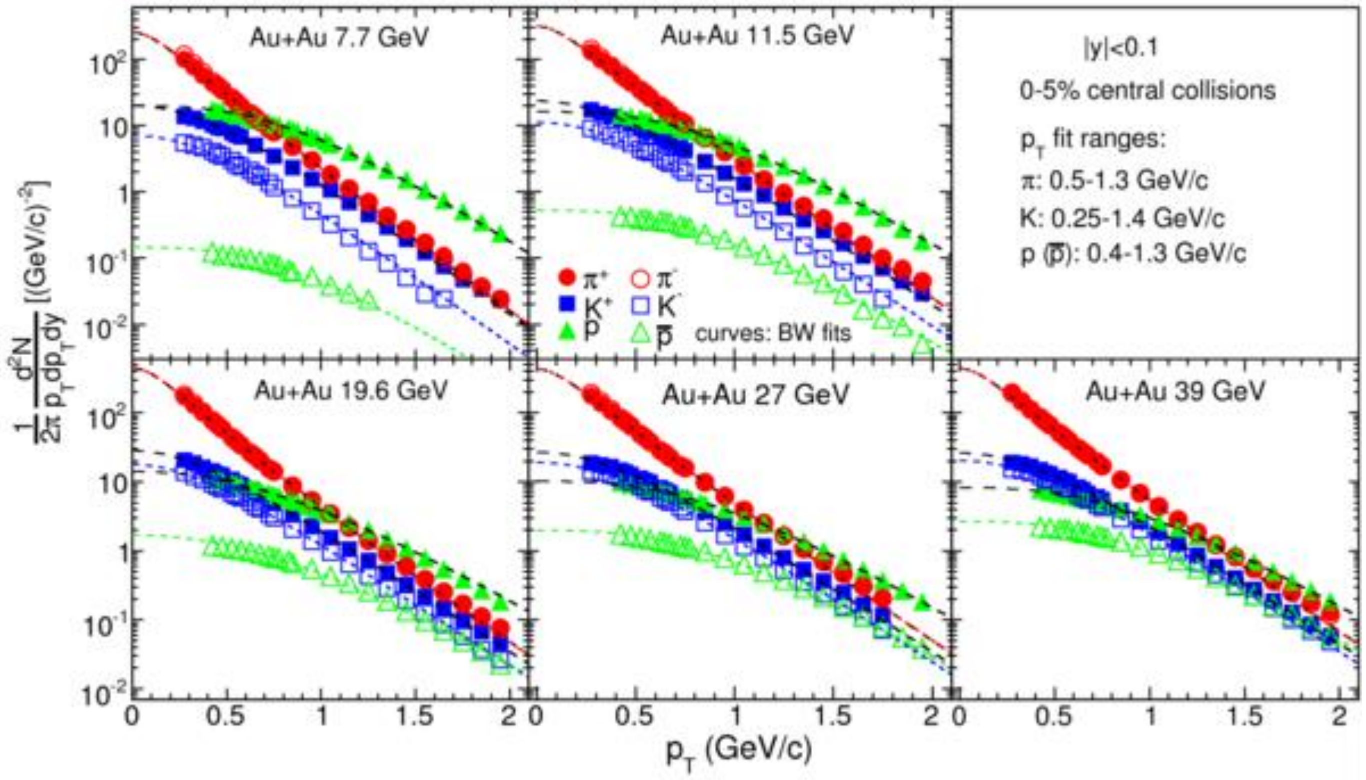

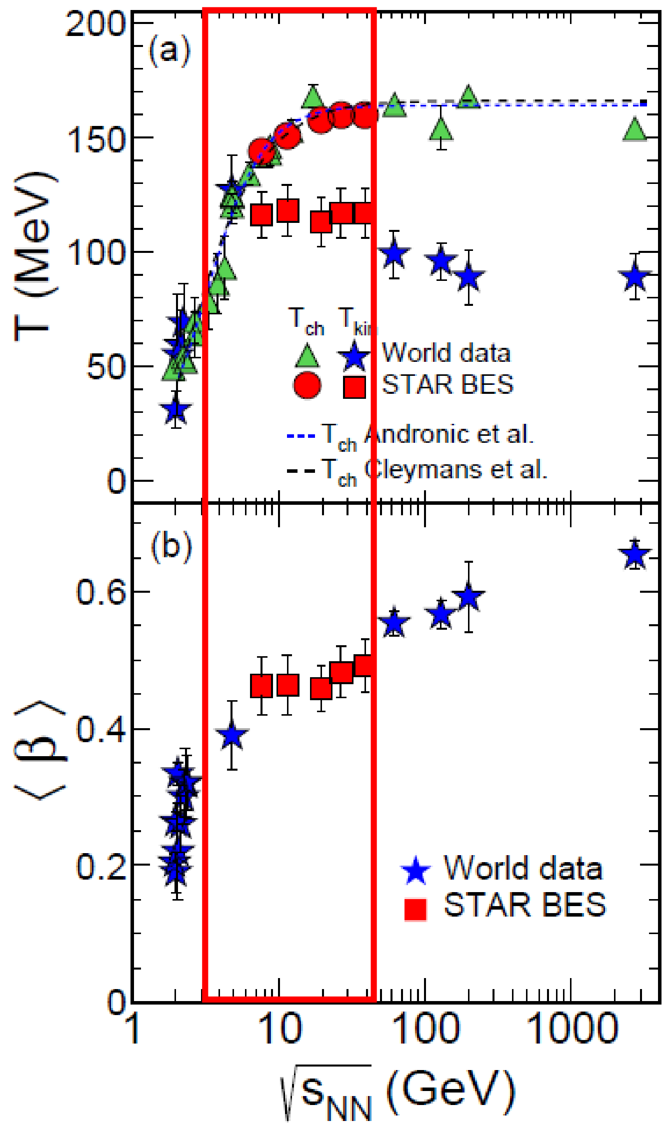

Parameters: Temperature (T_{kin}) and transverse radial velocity (β) obtained by fitting the momentum distribution of particles.

Comparison to thermal model predictions

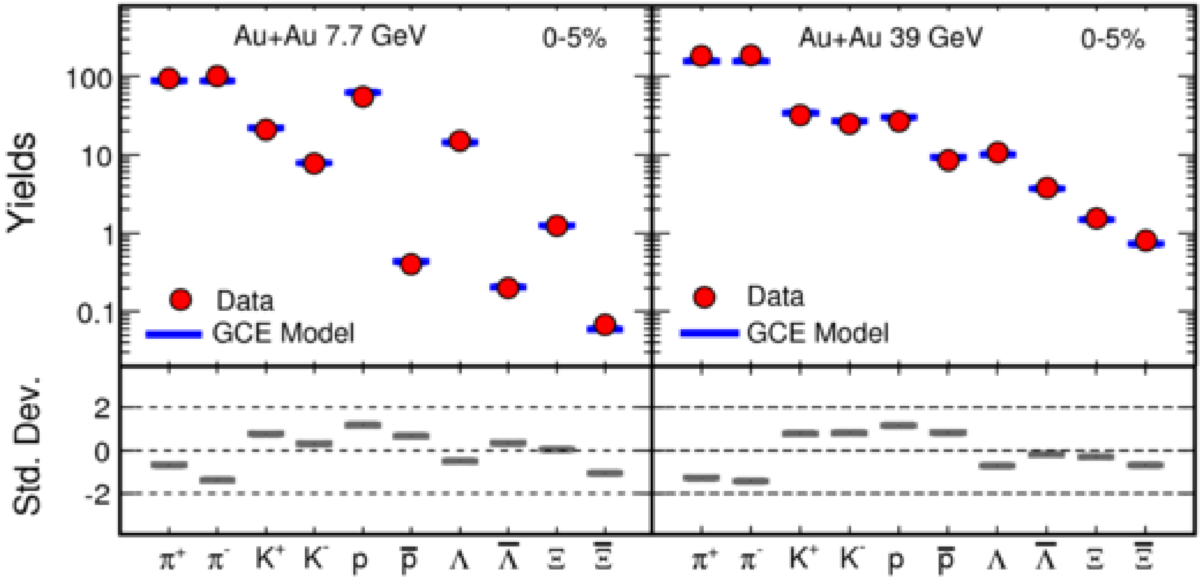

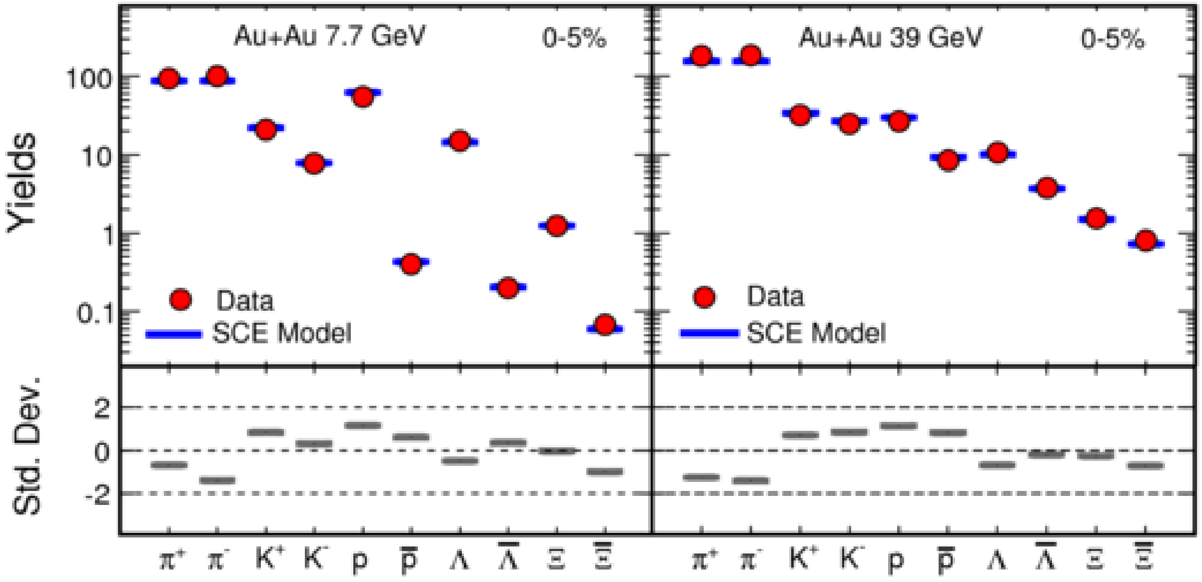

Blast-wave fits for particle spectra

$$\frac{d^2N}{2\pi p_T dp_T dy} \propto \int_0^R r dr m_T I_0\left(\frac{p_T \sinh\rho(r)}{T}\right) \times K_1\left(\frac{m_T \cosh\rho(r)}{T}\right)$$

Grand Canonical Ensemble – B, Q and S are conserved on average
Canonical Ensemble – exact conservation of B, Q and S
Strangeness Canonical Ensemble – exact conservation of S

Hidden vs. open strangeness production

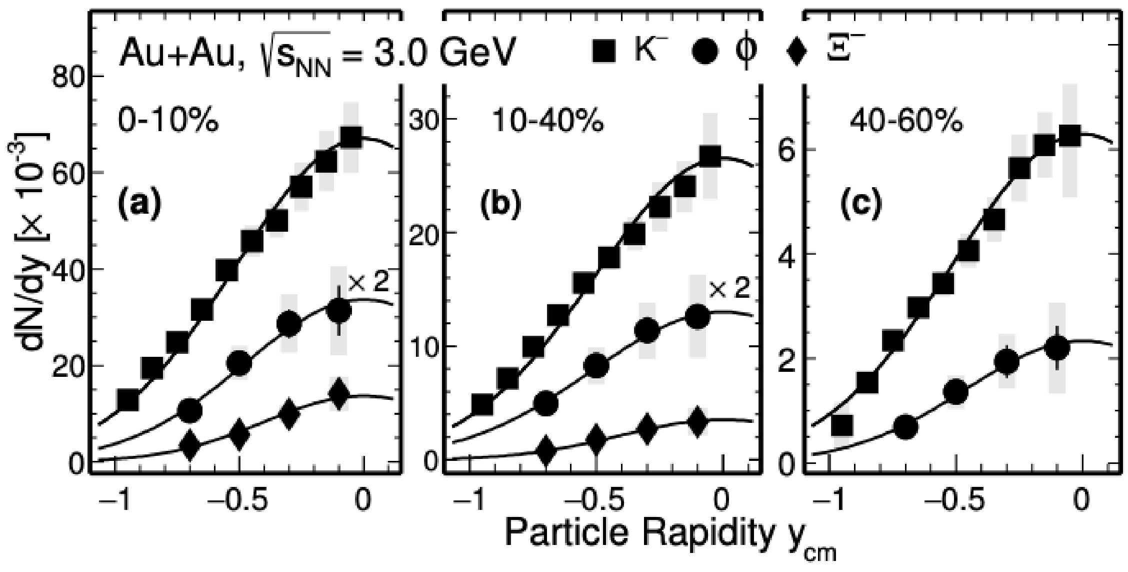

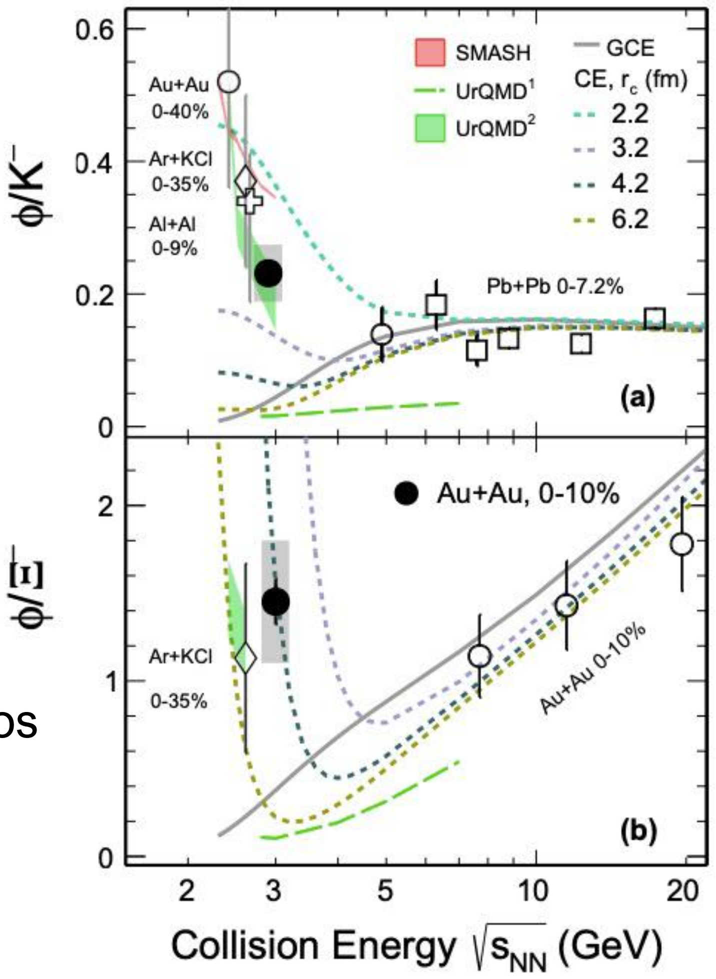

The thermal model with grand canonical ensemble (GCE) under-predicts the ratios

The canonical ensemble (CE) calculations reproduce the ratios with a correlation length of 3-4 fm

Phys. Lett. B **831**(2022) 137152

Dielectron production at 27 and 54.4 GeV Au+Au collisions

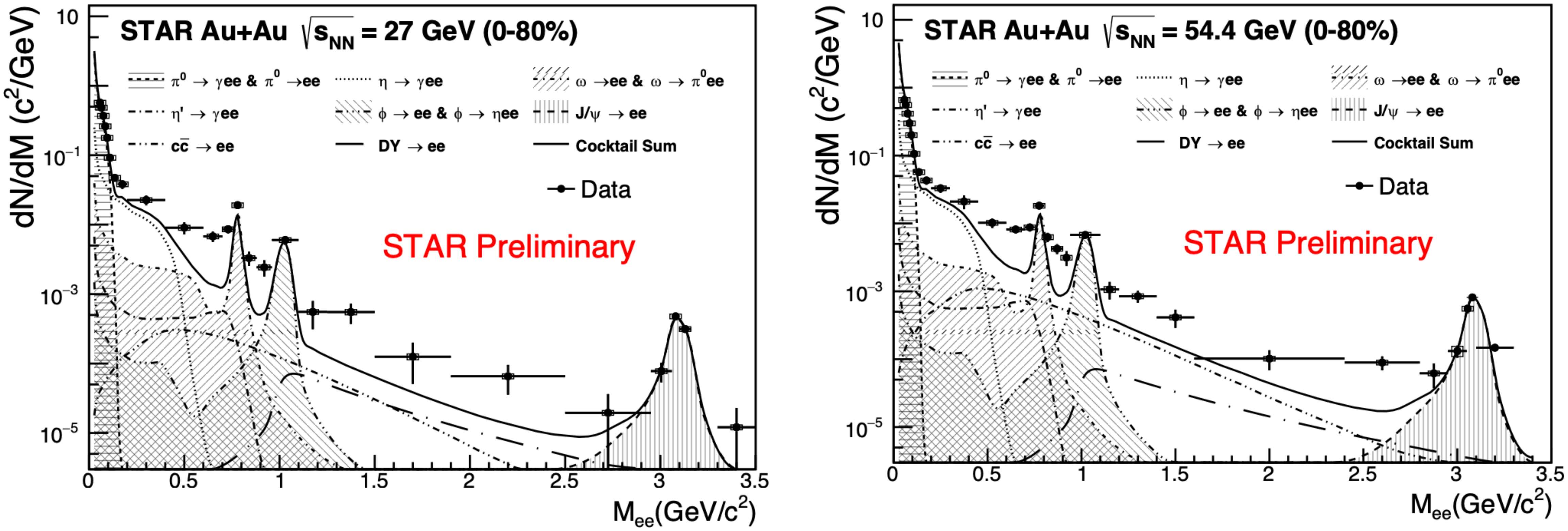

Clear enhancement compared to ρ excluded cocktail simulation in LMR and IMR

Thermal dileptons

Excess dielectron spectra in 27 and 54.4 GeV Au+Au collisions and NA60 In+In collisions are similar

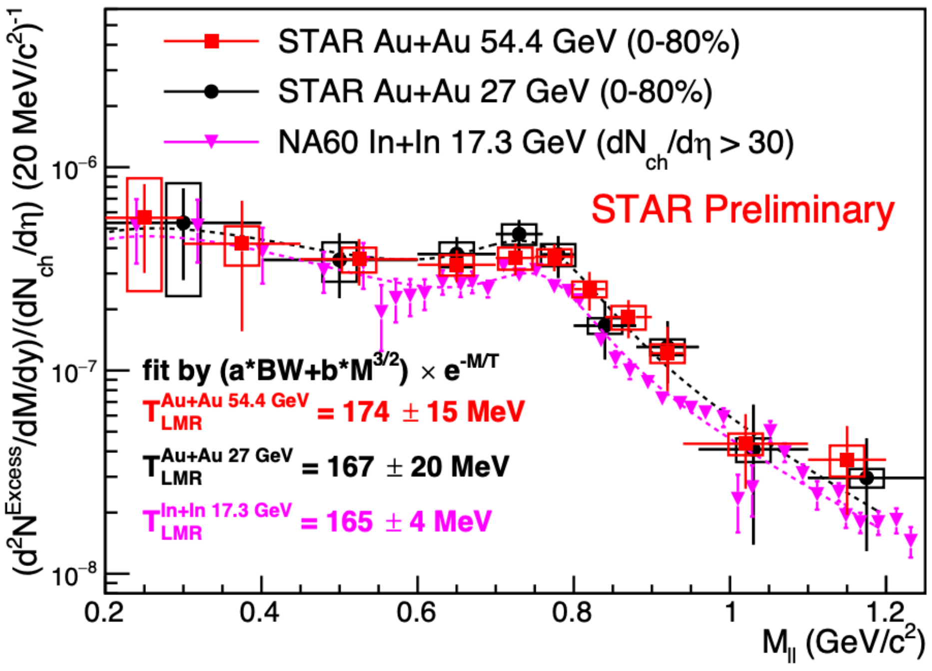

T extracted from low mass region around the pseudo critical temperature T_{pc} (156 MeV)

Thermal dielectrons is the major source in IMR

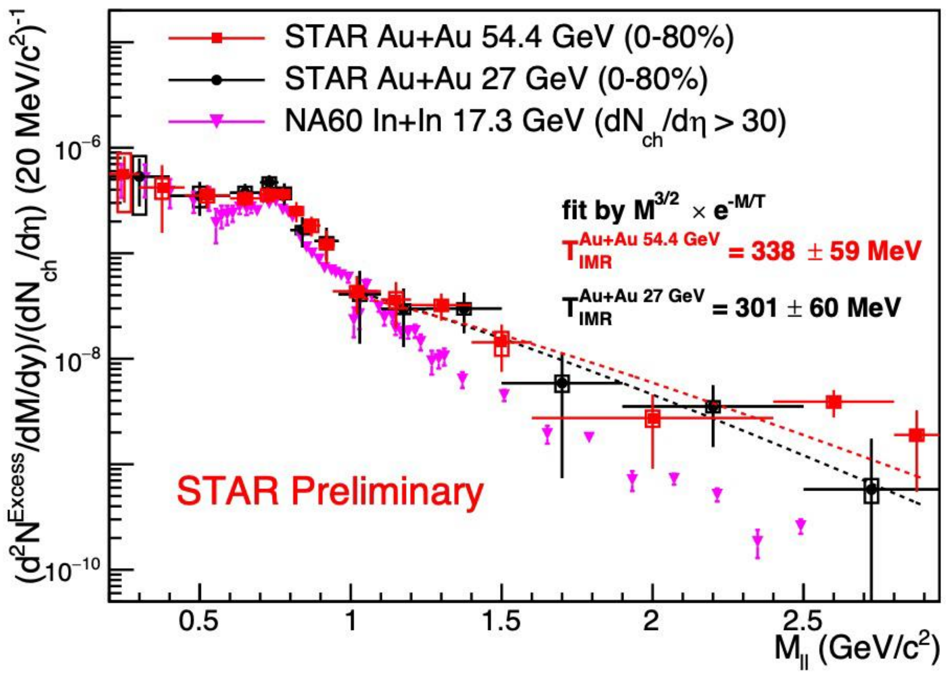

T in 27 and 54.4 GeV are consistent with each other

T > T_{pc} (156 MeV): emission dominantly from QGP

NA60: EPJC (2009) 59: 607–623
HotQCD: PLB **795** (2019) 15-21

Phase diagram mapping with dielectrons

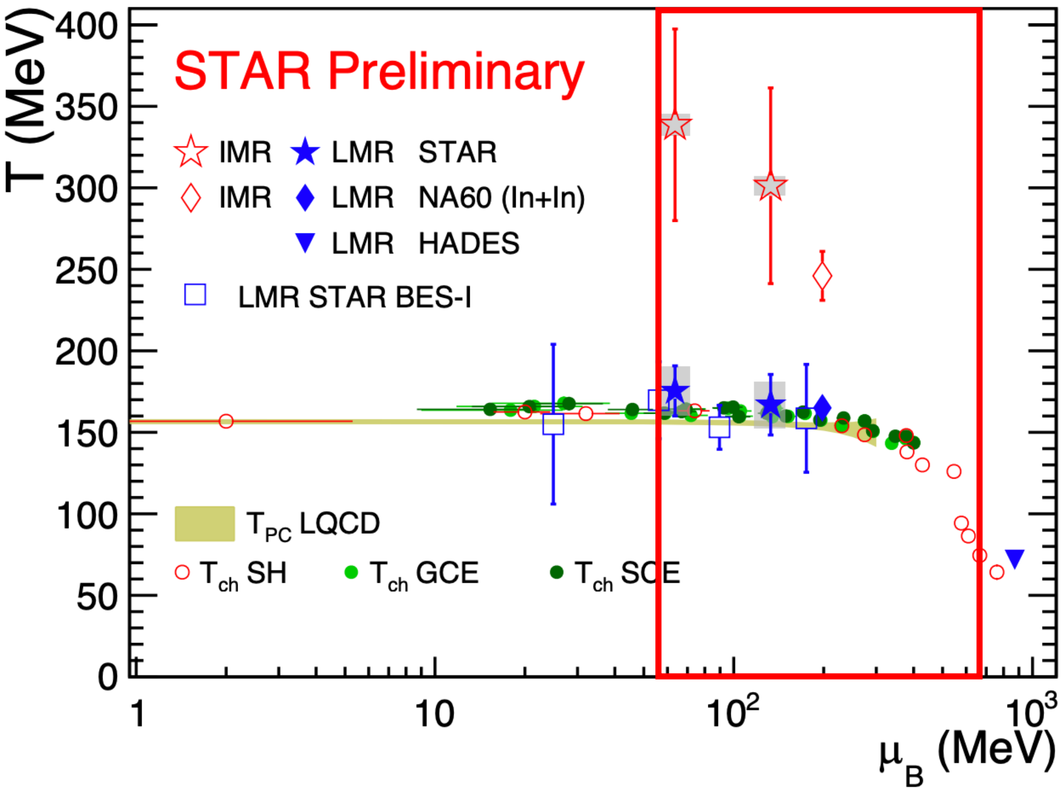

T_{LMR} close to T_{ch} and T_{pc}
ρ meson dominantly emitted around phase transition

T_{IMR} higher than T_{LMR}, T_{ch} and T_{pc}
dielectron dominantly emitted from QGP phase

High statistics data sample between 7.7 GeV and 19.6 GeV in STAR BES-II will help map the kink region

Enhanced tracking and particle identification capabilities with iTPC and eTOF upgrades

NA60: EPJC (2009) 59 607–623
HADES: Nature Physics 15, 1040-1045 (2019)
Tch SH: P. Braun-Munzinger et al. Nature 561, 321-330 (2018)
Tch GCE/SCE: STAR PRC **96**, 044904 (2017)

Higher-order cumulants at 3 GeV

Cumulants of proton and its ratios at 3 GeV

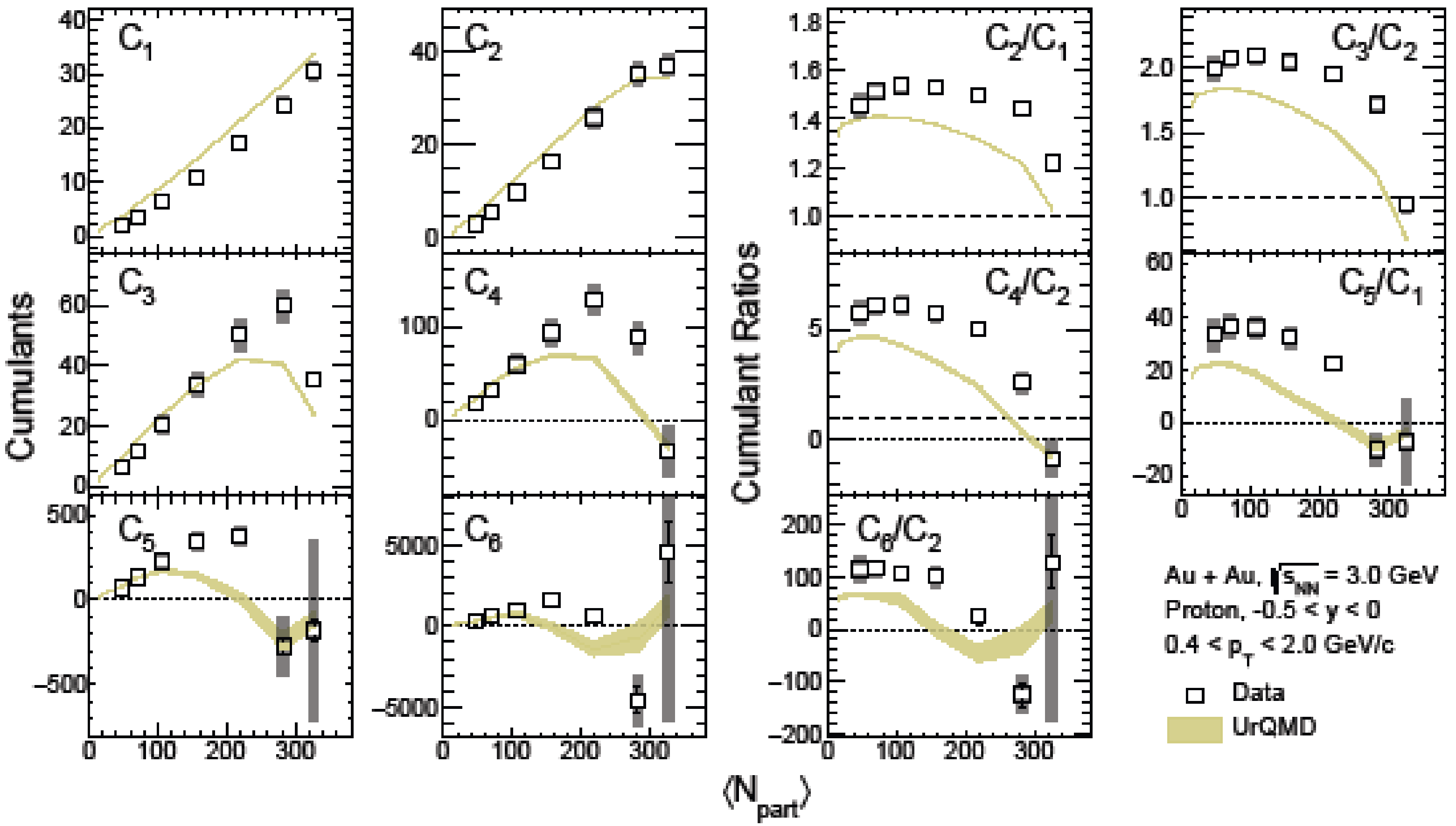

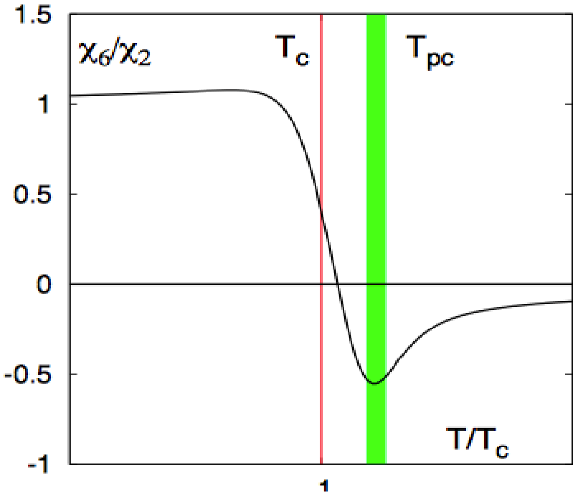

Susceptibility ratios fluctuate near the CP. It can be measured via cumulants of net-protons

$$C_1 = \langle N \rangle$$

$$C_2 = \langle (\delta N)^2 \rangle$$

$$C_3 = \langle (\delta N)^3 \rangle$$

$$C_4 = \langle (\delta N)^4 \rangle - 3\langle (\delta N)^2 \rangle^2$$

Higher-order cumulant ratios C4/C2, C5/C1, and C6/C2 in most central events appear least affected by volume fluctuations in the 3 GeV Au+Au collisions

e-Print: 2209.11940 [nucl-ex]

Energy dependence of net-proton cumulant ratio

Previous measurements of net-protons by STAR and HADES suggested the sign change at energies of BES-II

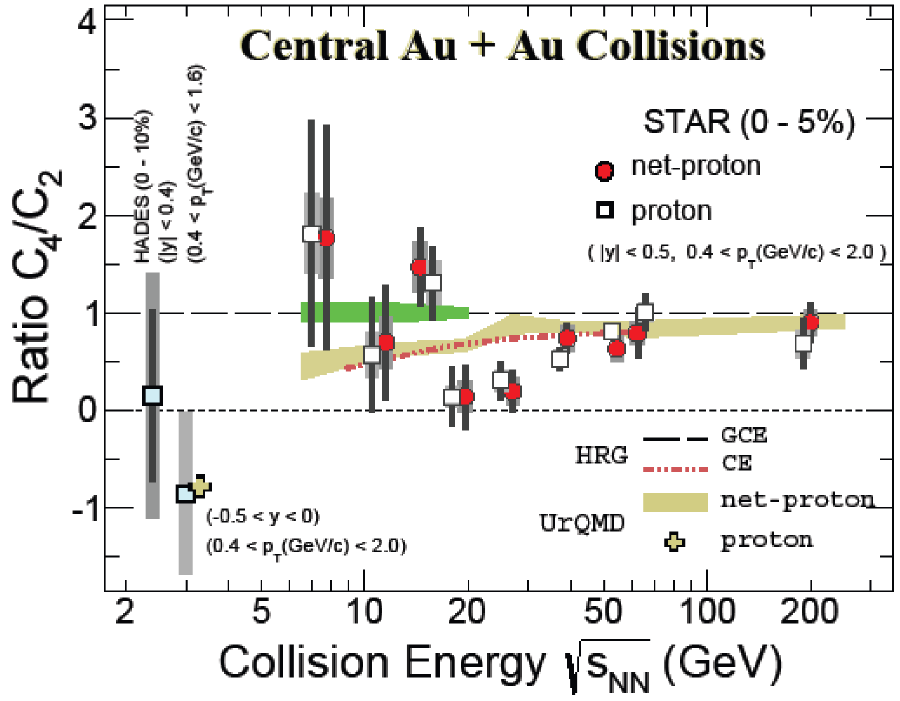

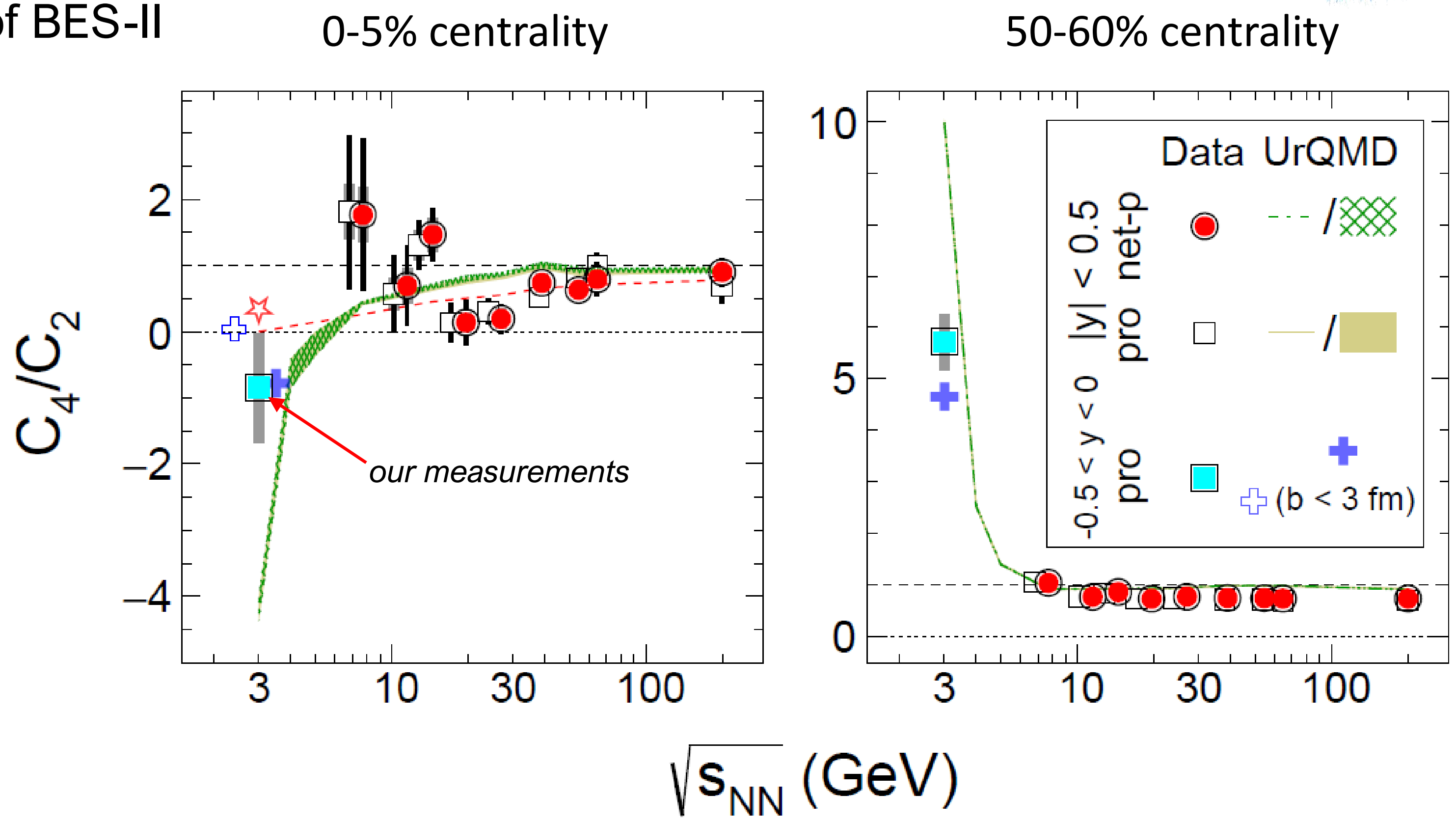

The data and results of both UrQMD and hydrodynamic models of C4/C2 in the most central collisions at 3 GeV are consistent, which signals the effects of baryon number conservation and an energy regime dominated by hadronic interactions